UNIVERSITÀ DEGLI STUDI DI PADOVA

Dipartimento di Ingegneria Industriale

Corso di laurea magistrale in Ingegneria Meccanica

Tesi di laurea

SELF - HEALING OF POLYMERS AND COMPOSITES BY THERMAL ACTIVATION

Relatore: Chiar.mo Prof. Marino QUARESIMIN

Correlatore: Chiar.mo Prof. Karl SCHULTE

Laureando: Enrico CHERUBINA
Matr. 623181

Anno Accademico 2012 - 2013

Abstract

The wide employment of composite materials in a great variety of several fields, if on one hand offers a series of peculiar advantages, these are paid on the other hand with a higher complexity in structure and in failure modes, affecting both the reinforcement and the matrix.

To face the problems resulting from matrix damages, in the last few years many solutions have been proposed and tested to create a resin with self-healing ability, for which the closure of cracks could occur with little or no external intervention. In this work, an overview of the most important techniques is given. Then, the research has been focused on the production and testing of a polymeric system in which a thermosetting resin and a healing agent are mixed in an homogeneous blend and which could be restored with the simple supply of heat.

After a failed attempt of employing an ionomeric polymer (Surlyn 8940) as healing additive, a self-repairing blend could be successfully obtained by mixing a set percentage of thermoplastic phenoxy resin to the thermosetting epoxy.

A series of specimens has been thus produced the ability of the material to close occurring cracks was analysed by means of Compact Tension tests. Particular attention has been given to the recovery percentage of one healing process and its variation with the heating process parameters.

Index

List of symbols

Symbol	*Measure*	*Description*
F	N	Force
δ	mm	Elongation, or displacement
σ_2	Pa (MPa)	Transverse tension, acting perpendicularly to fibres direction
G_{IC}	J/m^2	Critical Strain Energy Release Rate (SERR)
K_{IC}	$MPa\sqrt{m}$	Critical Stress Intensity Factor (SIF)
R_E	Adimensional	Material recovery in impact strength
R_E^0	Adimensional	Material recovery of pure resin
E_{heal}, E_{init}	Pa (MPa)	Impact strength for healed and virgin material
P_C	N	Load at failure
ε	Adimensional	Percentage error
h,w	mm	Thickness and width of Compact Tension specimens
m	Adimensional	Slope of a curve
$\bar{x}$	Dependent	Mean value
σ_x	Dependent	Standard deviation
N	Adimensional	Number of considered elements
R_1	Adimensional	Recovery ratio after the first healing action
V	V (mV)	Voltage
E	J	Fracture energy

List of abbreviations

CFRP	Carbon Fibres Reinforced Plastic
CNT	Carbon Nanotube
CT	Compact Tension
DA	Diels-Alder
DMA	Dynamic Mechanical Analysis
DSC	Differential Scanning Calorimetry
EMAA	Ethylene Methacrylic Acid
FPF	First Ply Failure
HGF	Hollow Glass Fibre
HM	High Modulus
HR	High Resistance
LEFM	Linear Elastic Fracture Mechanics
MA	Methacrylate
PCL	Poly(ε-caprolactone)
PIPS	Polymerisation-Induced Phase Separation
POM	Polarized Optical Microscopy
rDA	retro Diels-Alder
SEM	Scanning Electron Microscopy
SENB	Single-Edged Notch Bend
SERR	Strain Energy Release Rate
SIF	Stress Intensity Factor
TDCB	Tapered Double Cantilever Beam

Index of pictures

Index of tables

1 Introduction to composite materials

1.1 Applications and characteristics

In the last decades, composite materials have gained more and more popularity in a wide range of engineering applications, mainly due to the double advantage of presenting good mechanical properties and a lower weight when compared with traditional metallic materials. These features made these materials most suitable for fields in which mechanical structures need to be light as much as resistant (e.g. aircraft engineering). Though, the employment of composites brought the necessity to adopt completely new manufacturing processes, as long as to create new design methods to take into account the generally anisotropic behaviour. This characteristic is a direct consequence of the heterogeneous composition of such materials, whose simplest structure consists of a load-bearing element (fibres) and a binding and protecting element (matrix). This duality introduces the necessity of a design phase for the material itself, differently from what happens for the isotropic ones, in which the mechanical properties can be varied by acting on parameters as the fibres' percentage or orientation and the matching between different materials for the matrix and for the fibres.

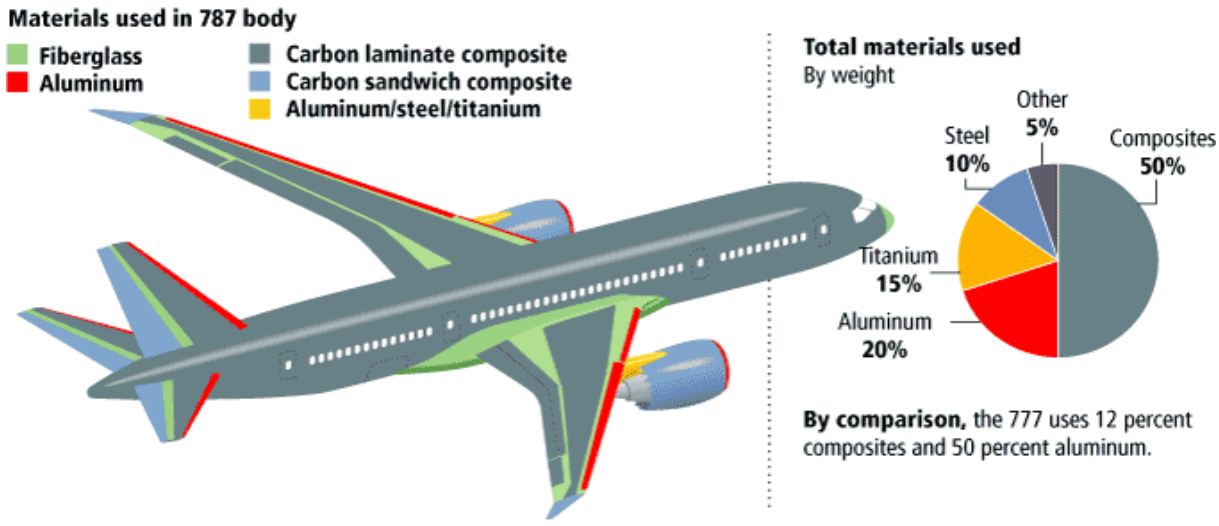

Figure 1.1: Comparison between the percentages of composites and metallic materials employed for the Boeing 787 Dreamliner [1].

1.2 Fibres

Mechanical properties such as tensile strength and stiffness of a composite material greatly depends on this constituent, whose function is to bear the loads acting on the structure. Different behaviours of the composite can be achieved by varying length and orientation of the fibres, or by using different materials. For synthetic composites, the fibres which are most commonly employed are of three types [2]:

- **Glass fibres**: available in E, R or S type, they are characterized by a high density and good strength properties, while generally lacking in elasticity. The low cost make them suitable for a wide range of applications, when very high performances are not required.
- **Carbon fibres:** combining a low weight to very good strength and stiffness, carbon fibres are widely employed in high-performance applications, e.g. the aeronautic field. High Modulus (HM) and High Resistance (HR) carbon fibres are available, the formers presenting however a much higher cost and being used only when stiffness is an essential requirement.
- **Aramid fibres:** the main characteristic of this kind of fibres is a great fatigue and impact resistance, which make them suitable for sport tools or ballistic armour. Though, the large employment for composites is impeded by manufacturing and impregnation difficulties.

1.3 Matrices

According to the purpose of keeping the fibres together, protecting them from environmental effects and distributing the applied loads, a good matrix should be characterized by relatively high mechanical properties, good adhesion and moisture resistance [2]. A main distinction can be done between thermoplastic resins, for which the solidification process is reversible, and thermosetting resins, which cannot be newly melted once the solidification has occurred. Virtually, any polymer can act as a matrix, though the most employed are basically four types of thermosetting resins. In the following lines, a short description of each is given, with a particular attention to the one used in this work (par. 1.4):

- **Polyester:** characterized by a very low cost, they present anyway quite poor mechanical properties and are thus employed for high volume manufacturing of low-performance products.

- **Phenolic:** like polyesters, phenolic resins present a low cost due to their intrinsic brittleness and to manufacturing problems. On the other hand, they have the advantage of a good fire resistance.
- **Epoxy:** epoxies are the most widely used resin, for the good mechanical properties and the high resistance to environmental effects. For the good performance which can be obtained, they are commonly employed as a matrix for carbon fibres.

It has to be noticed that the resin itself is only one of the components constituting the matrix: in fact, other elements can be added to ameliorate physical and mechanical properties, or to allow a easier manufacturing process. The following chapter illustrates the structure of the resin system employed in this work.

1.4 Epoxy matrix system

1.4.1 Epoxy resin

Taking the name from the presence in the chemical structure of the so-called "epoxide group" (see Fig.1.2), epoxy resins are one of the most common thermosetting materials for the production of prepregs and composites in general. Their wide employment is mainly due to the good mechanical properties (relatively high strength and modulus) and a low retirement during the curing cycle. If on the other hand there are the drawbacks of a rather high cost and the necessity of a good protection during processing, epoxy resins possess the additional advantages of a high degradation temperature, which ranges from 150 to 200 °C, and of being water resistant.

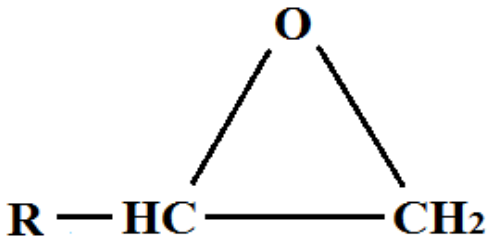

Figure 1.2: Epoxid group, also called "oxirane ring", characterizing epoxy resins [3].

1.4.2 Accelerators

Accelerators are common additives for epoxy systems, which allow a faster polymerization process enhancing the reactivity of the components. They represent a very small percentage of the whole system (usually from 3 to 5 % of the epoxy quantity) and are basically used for low-temperature applications. A slight change in mechanical properties such as stiffness and impact strength could also result from the utilization of such elements.

1.4.3 Hardeners, or curing agents

As the name suggests, these components are needed to confer to epoxies their effective mechanical properties, causing the cross-linking of the viscous and easy-to-handle state of the resin. Since the resin is a thermosetting one, the curing reaction is obviously irreversible and, depending on the nature of components, can be brought on at room temperature or at temperatures reaching 200 °C. To these element is related the “pot life” parameter, which indicates the amount of time available before the complete hardening of the mixture and is strongly dependent from the quantity of the cured resin and the processing temperature.

2 Damage evolution in composites

2.1 Damage modes

Damage evolution in composite materials has represented one of the most challenging fields in material science, due to the concurrence of many different factors influencing their behaviour. Nevertheless, progressive damaging occur in a wide range of composite applications (e.g. aeronautics, wind power generation, naval engineering) and thus many different studies have been carried on in order to properly understand and control these failure mechanisms.

As we know, the damage mechanism in metallic materials and in all the ones which manifest an isotropic behaviour is represented by the propagation of a single crack, enhanced by the application of an increasing load, which eventually reaches the dimension of the component itself and causes its failure. The different and greatly more complex behaviour of composites is basically due to their non-homogeneous and anisotropic behaviour, which brings final failure as the result of a series of separate and different types of damage [2]. Parameters affecting this behaviour can be the orientation of the fibres, the materials used for fibres and matrix or the lay-up of the laminas, that means the order in which the laminas are piled. It is then easy to understand the difficulties in creating a general failure model, since each composite laminate can virtually behave in a different way.

A distinction can be made between three different damage modes which occur within a single lamina and are thus called “intralaminar failures”:

- Breakage of the fibres to tension, compression or shear;
- Cracks within the matrix;
- Failure at the interface between fibre an matrix (debonding).

In addition to these, another type of damage affects the interface between two different laminas and causes their progressive separation: this is the so-called “delamination”, which is defined as an “interlaminar failure” (Fig.2.1).

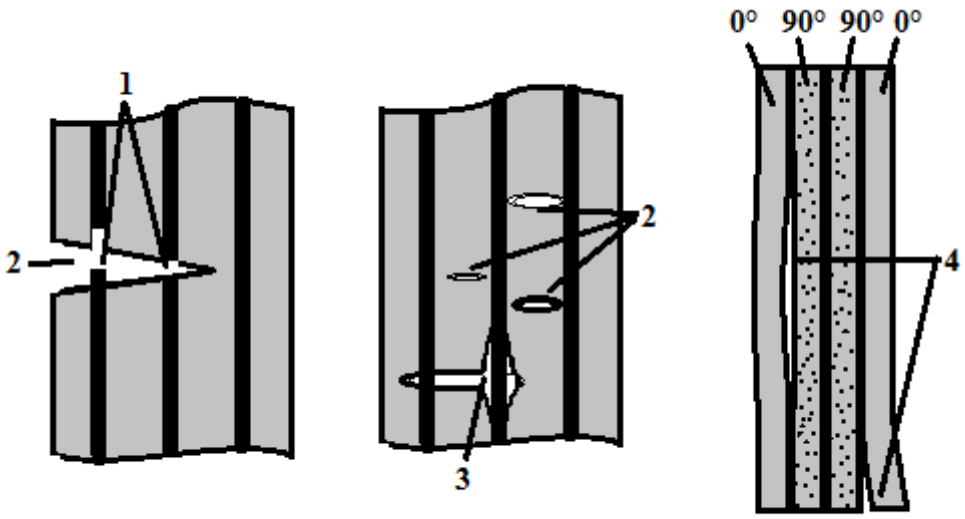

Figure 2.1: Damage modes for composite materials: 1. Fibre breakage; 2. Matrix cracking; 3. Interfacial debonding; 4. Delamination in a symmetrical cross-ply laminate.

2.2 Crack growth in a cross-ply laminate

Due to the heavy orthotropy of composite materials, their ultimate strength values are greatly influenced by the direction of the applied force. Thus, a laminate can maintain a specific bearing ability even after the breakage of some laminas, generally the ones in which the fibres orientation is orthogonal to the direction of the applied load. Depending on the strength of the interlaminar bond, a broken lamina can preserve part of its load-bearing properties,

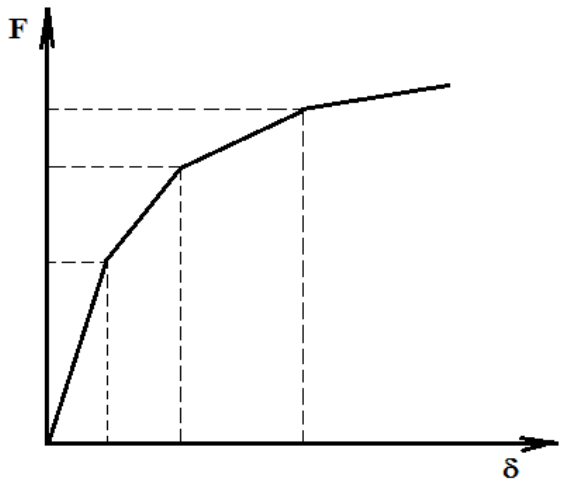

Figure 2.2: Typical force-elongation curve for laminates according to the First Ply Failure model (FPF). Each discontinuity represents the failure of the lamina and the subsequent loss in stiffness [2].

being only locally affected by the presence of the crack. Anyway, this behaviour is usually not considered in the traditionally adopted models (e.g. the First Ply Failure model, FPF), so that the contribution of a lamina after the appearance of a crack is assumed to be negligible [2]. The resulting relationship between an applied tensile load F and the elongation δ of the laminate can be schematized as shown in Fig.2.2, in which the discontinuities and different slopes of the curve represent the decreases in stiffness occurring after each breakage.

To better understand the mechanism of the damage evolution in composite materials, let's consider the case of a cross-ply symmetric laminate $[0/90]_S$ subjected to an increasing tensile force (Fig.2.3).

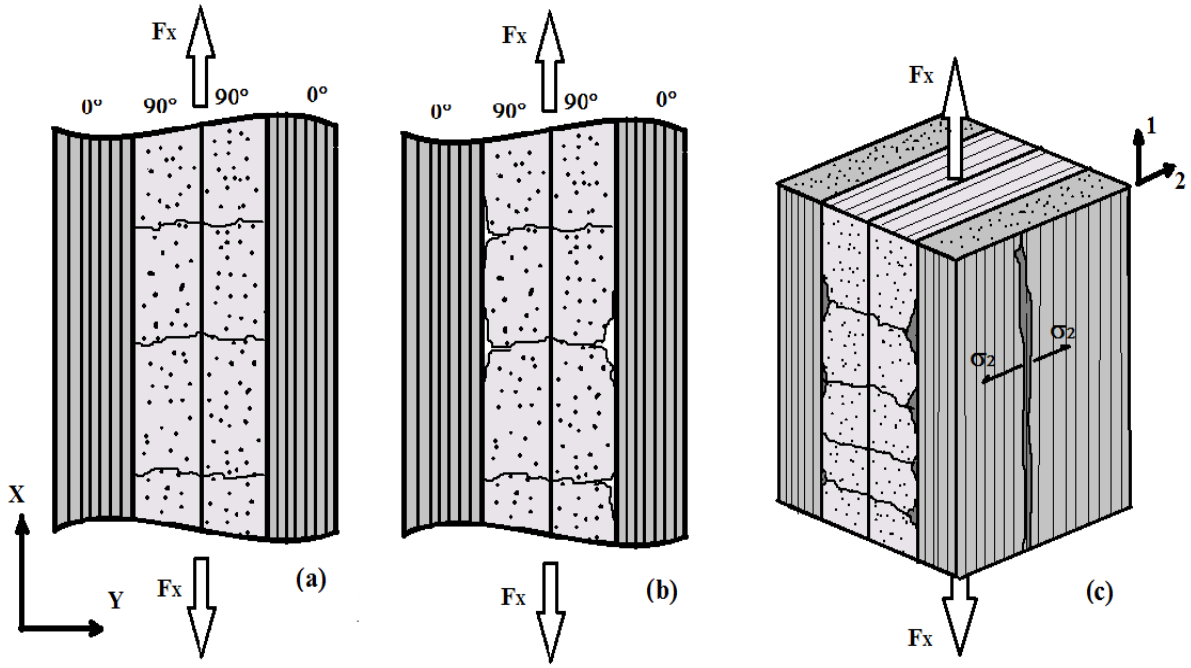

Figure 2.3: Typical damage evolution in a cross-ply symmetric laminate: (a) transverse cracking within the 90° oriented laminas; (b) delamination at the interface; (c) longitudinal splitting in the 0° oriented laminas.

As previously reported, the first crack occurs in the laminas with a fibres orientation of 90°, for which the tensile strength in the X direction is almost completely dependent on the matrix (matrix-dominated property) and is thus much lower than in 0° laminas. An increase in the load (a) brings the appearance of new cracks, generally nearly equidistant, and the progressive loss in stiffness of the laminate. It can be noticed that the crack path is not influenced by the interface between two equally oriented laminas, while it can be altered when reaching a differently-oriented lamina. The propagation is then depending on the strength of the interlaminar bond: if this is high, no further crack growth is possible and an increase in load causes the

creation of new cracks (a); a low bond strength involves a change in the crack direction and the subsequent damage follows the interface between the laminas (delamination, (b)), causing a redistribution of load on the 0° laminas. In these laminas, the behaviour of which is strongly fibre-dominated, the early damages can occur by breaking of fibres and partial debonding, as shown in Fig.1. A more evident effect of the stresses can be noticed in the final stages of the damaging process, in which the tension σ_2 acting in direction 2 (i.e. perpendicularly to the fibres orientation, according to the material coordinate system) eventually causes a longitudinal splitting (c) instantaneously propagating through the whole length of the laminate. The final breaking generally occurs by means of a transverse cracking extending on the whole thickness of the laminate.

2.3 Self-healing

It is clear that proper mending techniques are essential in order to avoid the catastrophic failure and extend the life of composite elements. Since, as can be stated from the previous paragraphs, the great part of the damage process occurs within the matrix, the possibility of an autonomic healing with no need of manual intervention could greatly enhance the reliability of the produced components. A composite with self-healing properties and based on thermal activation would allow time-consuming repairing techniques to be avoided and thus represents an important goal for modern material science.

3 History and theory of self-healing

In the last decade, many experiments were performed in order to reach a full knowledge of self-healing mechanisms and technologies, since in most of cases traditional methods for repairing composites were time consuming and expensive and required high skills usually difficult to achieve.

A manual bending of the damaged part, which is usually carried out by adding reinforcing layers or by injecting new resin in the crack, can only occur after an accurate inspection of the whole structure, in order to clearly localize the areas to be healed. It is thus obvious that the more internal the crack is, the more difficult the repairing process becomes. On the other hand, the simple replacement of the component is not acceptable, for it solves neither the time nor the economical problems.

For the reasons reported above, it is easy to state the advantages of a self-repairing behaviour, in which the healing action occurs with almost no human intervention and no need of an accurate localization of the damaged area, and which thus would represent a suitable solution for long-term high performances.

Since several analyses have been focused on finding an optimal solution for self-healing, many techniques are nowadays available in this field of study. According to Yuan et al. [4], a distinction can be made between extrinsic self-healing, in which the healing ability is conferred to the matrix using one or more external agents, and intrinsic self-healing, in which the matrix itself is able to heal the cracks with no need of pre-embedded devices.

In the following chapters, a review will be presented of the most common solutions, with particular attention for the one used in this work.

3.1 Extrinsic self-healing

As stated above, extrinsic matrices have no self-healing characteristics themselves, so that there is the need for an external agent to be added. As it will become clear in the further de-

scriptions, these techniques result from attempts to mimic the behaviour of biological systems like, for example, the human skin. The effective mechanism involved in healing of wounds is far too complex to be replicated, although the bleeding action has been satisfactory approximated by using special carriers which release the molten healing agent in the formed crack. The simultaneous release of a hardener allows then the solidification of the agent, and so the healing action, to occur. In the following lines, a short description of the most common extrinsic methods is given.

3.1.1 Microcapsules

This solution was first developed by White et al. [5] as a first attempt to create a smart material with autonomic healing properties. The healing agent is contained in special microcapsules which are incorporated in the base polymer and it is thus released when a crack causes the rupture of the jacket. For the healing to occur, it is also necessary to add the matrix with a catalyst which acts as a chemical trigger for the polymerization of the healing agent. The healing process is represented in Fig.3.1: **a** and **b** show the propagation of the crack in the modified matrix and the rupture of the capsules which release both the healing agent and the cata-

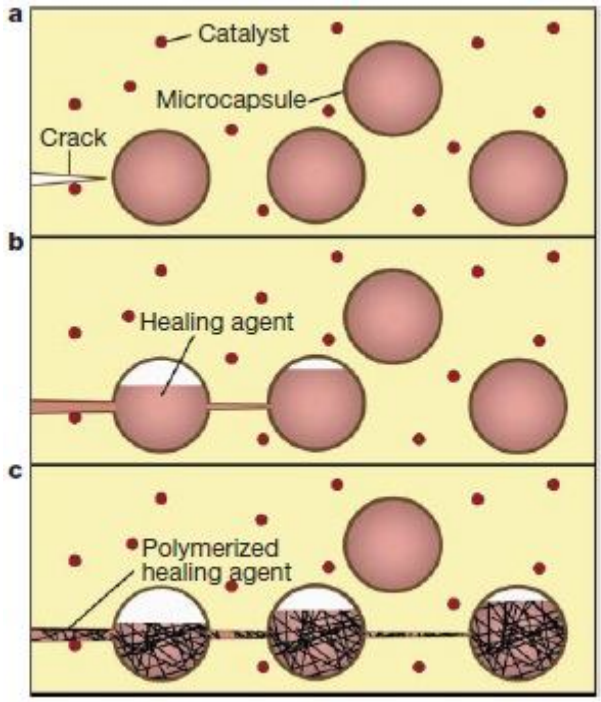

Figure 3.1: Microcapsules self-healing mechanism: a) Internal structure of the modified matrix; b) Filling of the crack following the rupture of the capsules; c) Polymerization and healing, as a result of the catalyst's action [5].

lyst; for the healing to occur (**c**), a good distribution of the capsules in the base polymer is essential.

The research was then focused on the polymerization chemistry, in order to optimize the action of the catalyst. Further studies [6] brought on the analysis of the healing process by testing several types of catalyst, in order to find an optimal solution. Object of testing were also the capsules' material and strength. In fact, since the jacket must resist to the manufacturing process and only break in consequence of a crack, a proper choice of the encapsulating material is essential for the healing process to succeed. To the same objective were directed the experiments performed by Keller and Sottos [7].

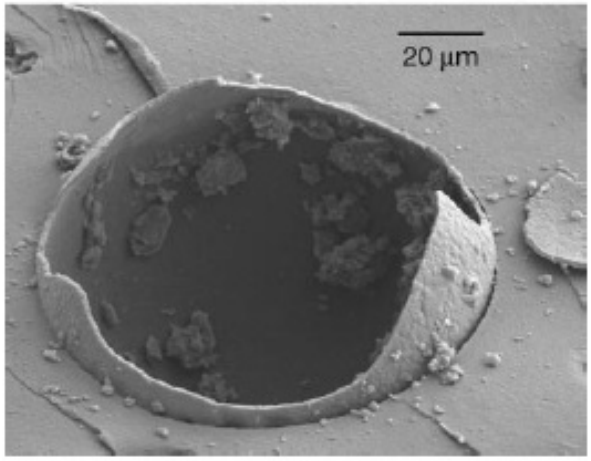

Figure 3.2: SEM image of a ruptured capsule [5].

Although some of the mechanical properties of the material seem to be enhanced by the modification with microcapsules [7], this self-healing technique involves a series of difficulties, mostly related to the manufacturing process. In addition to the problem represented by the production of liquid-filled hollow capsules, it is essential to provide for them a perfect dispersion in the base polymer, to prevent the propagation of unhealed cracks. Also, there is the need to accurately estimate the optimal thickness for the capsule walls in order both to avoid breaking during the manufacture process and to allow it when a crack occurs. For what repeatability is concerned, at date there is no way to predict a trend in the healing efficiency, since the quantity of unpolymerized agent after one healing action remains unknown. Finally, when used to create a self-healing composite, microcapsules could provoke waviness of the fibres, altering the chosen architecture: for this reason, the dimensions must be reduced as much as possible, necessarily involving new manufacturing problems.

3.1.2 Hollow glass fibres (HGF)

Another attempt to reproduce the biological healing was performed in 2001 by Bleay et al. [8], continuing the research formerly brought on by Dry et al. [9] for concrete. The healing agent and the catalyst are contained in hollow glass fibres and, similarly to how happens for microcapsules, they are released in the base material when a propagating crack breaks the walls of the containing body (Fig.3.3). This solution is somehow preferable to microcapsules, since the glass fibres act both as containers for the healing agents and as reinforcement for the composite. In addition, no alteration of the reinforcing fibres occurs because of the insertion of this device, while capsules, as mentioned above, can introduce a waviness effect which alters the mechanical properties of the composite. As experimented in the work of Pang and Bond [10], some fibres can be filled with a fluorescent dye in order to easily locating and highlighting the damaged area. Impact response of HGF reinforced plastic was investigated by Motuku et al. [11], who analysed the influence of parameters such as the specimen thickness or the distribution of the fibres.

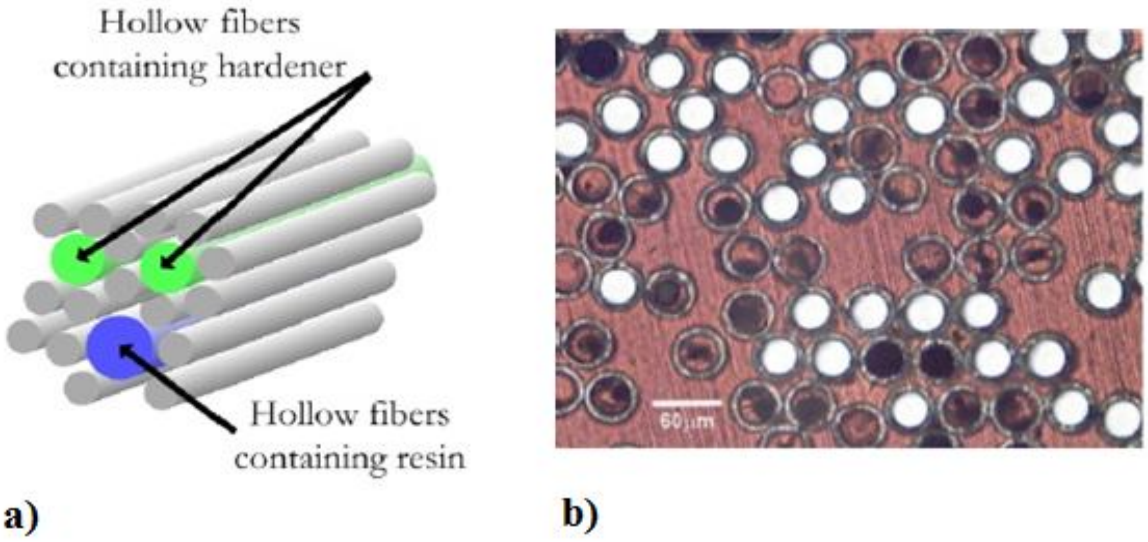

Figure 3.3: a) Disposal of hollow glass fibres within a composite material for achieving a self-healing behaviour [12]; b) Optical micrograph of hollow glass fibres [10].

However, also this solution necessarily involves several problems: according to the same studies, for example, the flexural stiffness of a composite laminate seems to be badly affected by the introduction of the hollow fibres, even if an increase in the life of the material was observed. Also, the use of glass fibres in CFRPs must be considered carefully, since it could heavily reduce the mechanical benefits provided by carbon fibres: in recent studies, Bond et al. [13] experimented how HGF's spacing and disposition affect the mechanical properties of

a CFRP specimen. The manufacturing problems presented for microcapsules also affect glass fibres, as the risk of breaking during the fabrication process is much greater, and there is obviously the need for the fibres to break when the propagating crack reaches them.

3.1.3 Microvascular 3D network

A few words must also be spent on the solution firstly introduced by Toohey et al. [14] and then further analysed in several researches [15], in which the healing agent is conveyed to the crack using a network of microchannels. The network is usually created using fugitive scaffolds around which the resin is formed. The subsequent removal of the scaffolds leaves a series of hollow channels inside the resin structure (Fig.3.4), allowing the filling with healing agent. This mechanism, which is a clear attempt to reproduce the human veins system, partly solves the repeatability problems, since the healing agent can be periodically injected in the network using an open, main channel running close to the material surface. On the other hand, this solution involves some restrictions on the choice of the matrix, since not all of them can be formed around fugitive scaffolds. Additionally, a close attention must be paid to the viscosity of the liquid healer, since a wrong evaluation can bring to the obstruction of the channels and so affect the long term reliability of this solution.

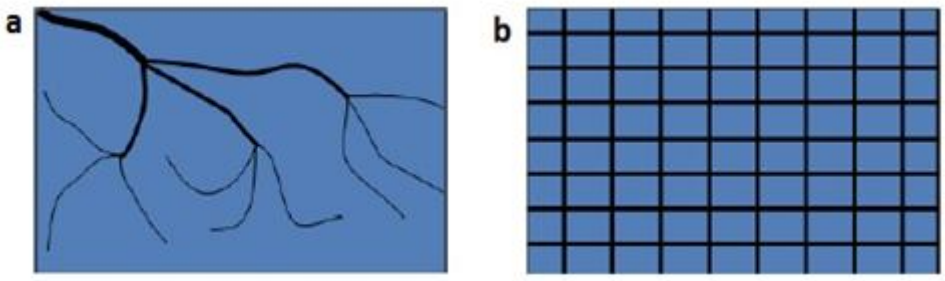

Figure 3.4 Different solutions for the network structure: tree arrangement (a), grid arrangement (b) [12].

3.2 Intrinsic self-healing

Using a matrix with self-healing properties allows many manufacturing problems to be avoided, since there is no need to introduce an external healing agent in the crack site. As seen in the previous paragraphs, in fact, the presence of microcapsules or other bio-inspired, extrinsic healing devices can provoke a distortion (waviness) in the orientation of fibres or in other ways involve heavy detrimental effects on the mechanical properties of the composite material.

In the latest years, this goal has been achieved and studied in many different ways [15]: a short description of the most common methods is given below. Being this work based on a thermoplastic-modified epoxy matrix, particular attention will be given to the correspondent part.

3.2.1 Reversible reactions

The use of materials with these particular reactions is based on the possibility to create and destroy the linkages between monomers in a reversible way, triggering the reaction by means of an external energy, usually heat. Thus, a damaged composite can be healed by a cycle of heating and cooling, in order to firstly separate the polymers in monomers with increased mobility and to successively recreate chemical bonds in the cracked area. The most common scheme used to the purpose is based on the Diels-Alder reaction (DA) and the inverse process, the retro-Diels-Alder reaction (rDA), (Fig.3.5). The possibility to create self-healing materials by means of this process was first demonstrated in 2002 by Chen et al. [16] for a furan-maleimide polymer. In a subsequent research [17, 18], the same polymer was added to an epoxy matrix as a trigger for the self-healing action.

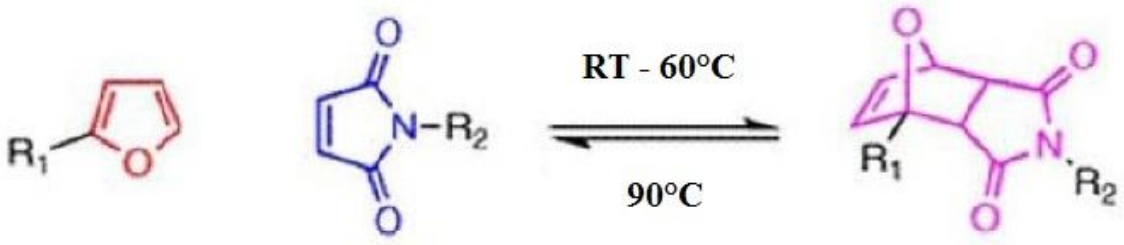

Figure 3.5: Diels-Alder reaction for a furan-maleimide polymer [16].

3.2.2 Thermoplastic additives

This method is based on the possibility to create a hybrid matrix by dissolving a specific percentage of thermoplastic resin, which acts as healing agent, in the basic thermosetting component. In the resulting blending, no phase separation must be detected, since the healing agent must be uniformly distributed in the matrix.

The auto-repairing action occurs by means of a heating operation: once surpassed a specific temperature threshold, the weak bonding between thermosetting and thermoplastic resin break, allowing the latter to diffuse throughout the matrix without any melting of the material and to fill in the cracks. A subsequent cooling enables the creation of new linkages between the components and a resulting healing in the damaged area.

The influence of parameters as the proportion between components or the healing temperature has been investigated by Hayes et al. [19,20,21], in order to finally produce a glass-fibre composite material with self-healing properties. The analysed material is a mixture of epoxy resin and poly(bisphenol-A-co-epichlorohydrin), the latter being dissolved in the matrix in a percentage varying from 5 to 20 wt%. This resin system was subjected to a series of Compact Tension (CT) and Charpy tests, each of whose was followed by heating and moving together the two obtained halves of the specimen. New tests performed on the so repaired specimens proved the effectiveness of the adopted resin system, since up to the 66% of the tensile strength could be restored. A similar trend could be detected in the CT tests for the strain energy release rate G_{IC} and for the stress concentration factor K_{IC} at failure. In addition to the obvious connection with the healing agent percentage (which leads to further considerations about the optimal quantity), the efficiency of the healing action has shown to be also related with the heating temperature, since higher values brought a better recovery of the mechanical properties.

A different approach to this healing mechanism was attempted in a later study by Luo et al. [22]. Though the underlying principle is basically the same, the blending produced mixing poly(ε-caprolactone) (PCL) and epoxy resin was structurally different from what previously reported. In fact, while in the first case a good dispersion of the healing agent in the matrix was to be achieved, this later research was focused on the creation of a biphasic structure (the so-called “bricks and mortar” morphology, see Fig.3.6) by means of the polymerisation-induced phase separation (PIPS). The resulting material is a resin in which the healing agent (PCL) interpenetrates and binds together a net of spheres of the major phase (hence the name “bricks and mortar”).

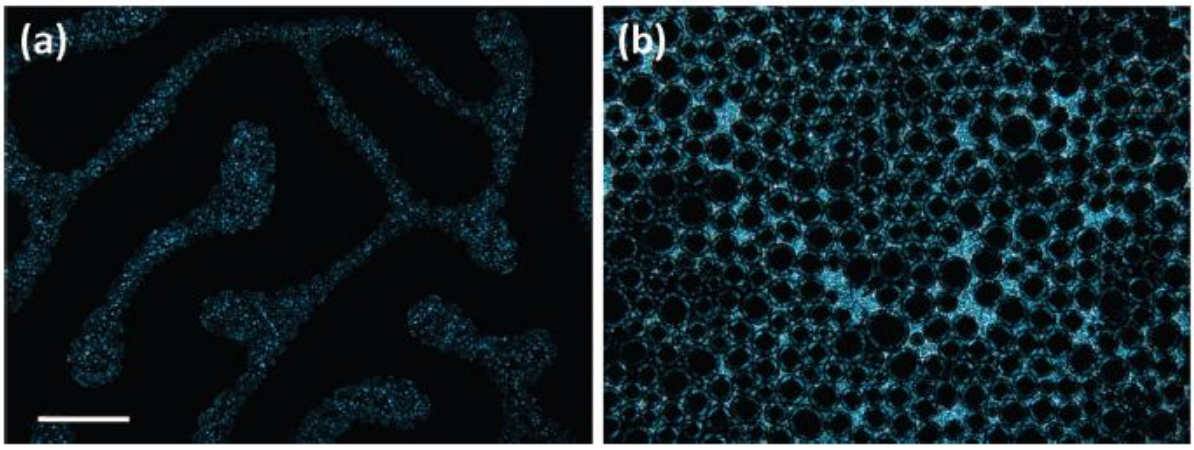

Figure 3.6: POM images for (a) epoxy/PCL(11.5) and (b) epoxy/PCL(15.5). The scale bar represents 200 μm [22].

Again, different concentrations were tested in order to find the optimal condition and the healing efficiency was evaluated performing fracture tests on single-edge-notched-beam (SENB) specimens. The results, though varying witch the PCL concentration, showed an excellent thermal mending ability, since the mechanical properties were in greatest part restored.

3.2.3 Ionomeric clusters

According to the definition given by Tant and Wilkes [23], "the term 'ionomer' represents any polymeric material that possesses 15 mol% or less of an ionizable species". In a subsequent research [24], they have been described as "polymers in which the bulk properties are governed by ionic interactions in discrete regions of the material". In other words, ionomers are random copolymers in which part of the internal structure consists of a ionic group and they can be obtained from copolymers by a neutralization process.

An interesting property of ionomers, which makes them suitable as healing agents, is a tendency to aggregate in the way shown in Fig.3.7.a. The ionic group, highlighted in blue, forms the so called "multiplet", while the red circled area represents a restricted mobility area constituted by the copolymers' chains. If the ionic concentration is sufficiently high, the restricted mobility areas of the single aggregates overlap generating larger areas called "clusters" (Fig.3.7.b).

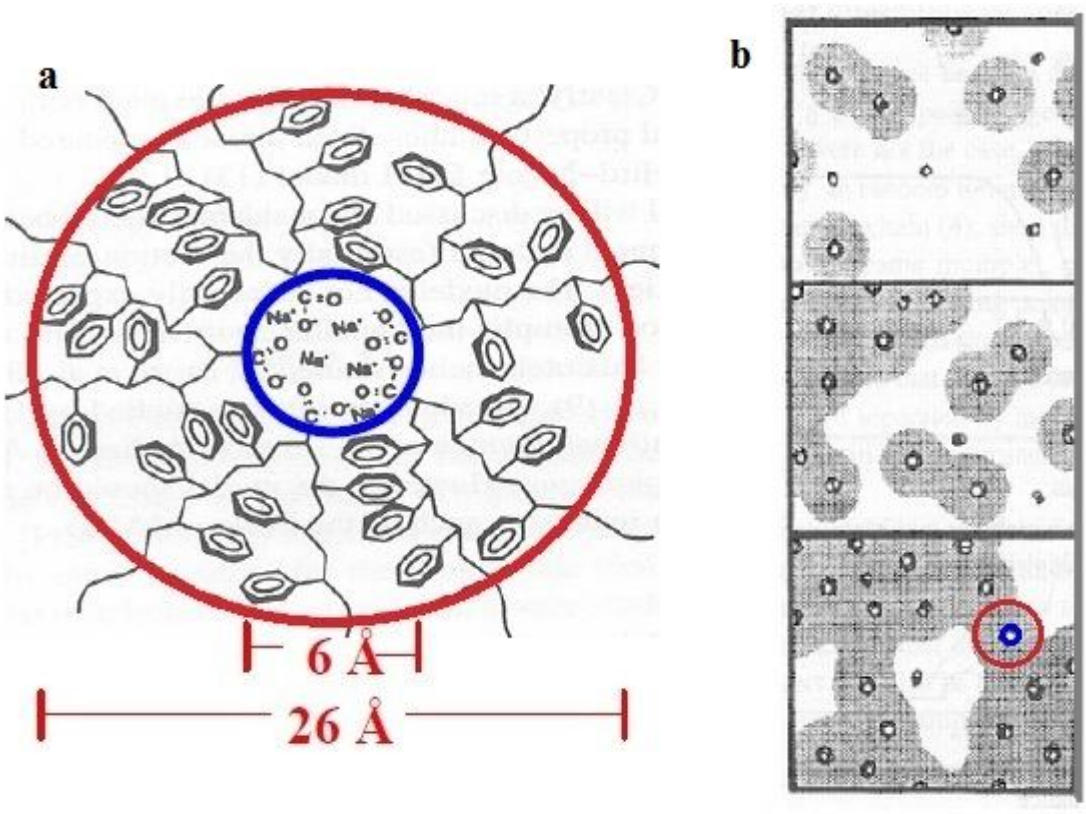

Figure 3.7: (a) Schematic representation of a restricted mobility area generated by aggregating ionomers; (b) Creation of clusters subsequent to a relatively high concentration of ionomers [25].

The reversibility of this process has been analysed by Tadano et al. [26], who investigated the particular behaviour of ionomers when a specific value of temperature, called “order-to-disorder temperature”, is reached. When the polymer is heated over this threshold, although the restricted mobility regions still persist, the polymer chains greatly increase their mobility an can migrate from one region to another, the so called “ion hopping”. This phenomenon, united to the reversible nature of the order-to-disorder process, represents the basis of the ionomers’ self- healing ability and can thus be applied in order to avoid or stop the propagation of cracks in the material.

The healing response of ionomers to impact damage was firstly inspected by Fall [27] and Kalista [28]. Further researches brought on by Varley and van der Zwaag [29,30] were then focused on the synergic action of different healing mechanisms, such as elastic and viscous response. All the mentioned tests were performed on a partially neutralized poly(ethylene-co-methacrylic acid) random ionomer co-polymer (EMAA). For the healing to occur, no further heat sources were necessary, since the heat generated by friction was a sufficient trigger to the reaction.

3.3 Evaluation of the healing ability

The ability of a matrix to heal occurring cracks has been investigated and delineated in several ways and performing a series of different tests on specimens of various shape. Though there is not a unique way to approach this task, the simplest procedure is to define a "healing efficiency" as the ratio between a specific measured property as it results from a healed specimen and the same property as measured on a virgin specimen (Eq.3.1):

$$\eta_{healing} = \frac{strength\ of\ healed\ specimen}{strength\ of\ virgin\ specimen} \qquad (3.1)$$

3.3.1 Charpy test

One of the possibilities reported in literature is to use the impact strength of the resin as evaluating parameter for calculate the healing efficiency. In the work of Hayes et al. [20], the previous formula has been expressed in a similar way:

$$R_E = \frac{E_{heal}}{E_{init}} \cdot 100 \qquad (3.2)$$

where: R_E is the recovery of the material,

E_{heal} , E_{init} are the impact strengths respectively after and before the healing action.

Since the pure resin can present some slight healing action itself, a precise calculation should be done in consideration of this behaviour. Equation *3* shows how an accurate value of the healing efficiency can be obtained subtracting the recovery of the pure resin R_E^0 to the result of Equation *2* [20]:

$$\eta_{healing\ (E)} = R_E - R_E^0 \qquad (3.3)$$

The values of the impact strength can be determined using a Charpy specimen, which represents the easiest and fastest way to test this property due to a relatively easy preparation. Common dimensions for a this kind of specimens are reported in Fig.3.8:

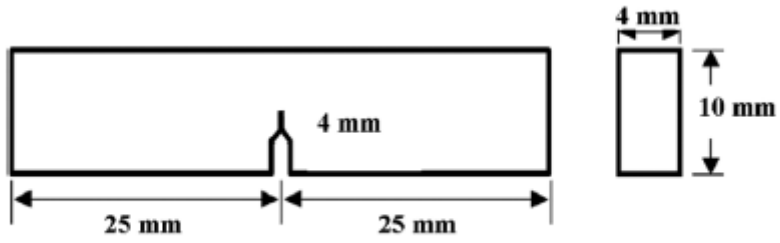

Figure 3.8: Dimensions for a Charpy specimen as used in [21].

The test consists in breaking a resin specimen using the Charpy pendulum and immediately rejoining the two halves applying a slight pressure and supplying heat (for the healing action to occur, it is essential a perfect alignment of the broken parts). After a set heating time, the specimen is subjected to a second test and the new impact behaviour data are taken and compared. This process can be iterated in order to obtain some information about the repeatability of the phenomenon.

3.3.2 Compact Tension test: CT specimen

Despite the simplicity of the test reported above, a more common way to evaluate the healing efficiency considers the decrease in linear elastic fracture toughness after breakage and subsequent mending and compares it to the initial condition of the material. Eq.3.1 can thus be written as follows:

$$\eta_{healing\ (K)} = \frac{K_{IC\ healed}}{K_{IC\ virgin}} \qquad (3.4)$$

According to the theory of linear elastic fracture mechanics (LEFM), K_{IC} is the threshold for the Stress Intensity Factor (SIF) K at which a crack subjected to an opening stress (hence the subscript I) begins to propagate. An analogous ratio can be defined for the Strain Energy Release Rate (SERR), symbolized by G, with the determination of the efficiency $\eta_{\ healing\ (G)}$.

These factors can be obtained by means of a Compact Tension (CT) test, in which a specimen shaped as in Fig.3.9 is subjected to a tensile stress to finally achieve an opening mode (I) fracture. The procedure follows then what reported in Par.3.3.1: after an accurate re-alignment of the two halves, the specimen is heated (the temperature adopted and the duration of the heating process have been proven to influence the efficiency of the healing action) and subsequently a new CT test is performed.

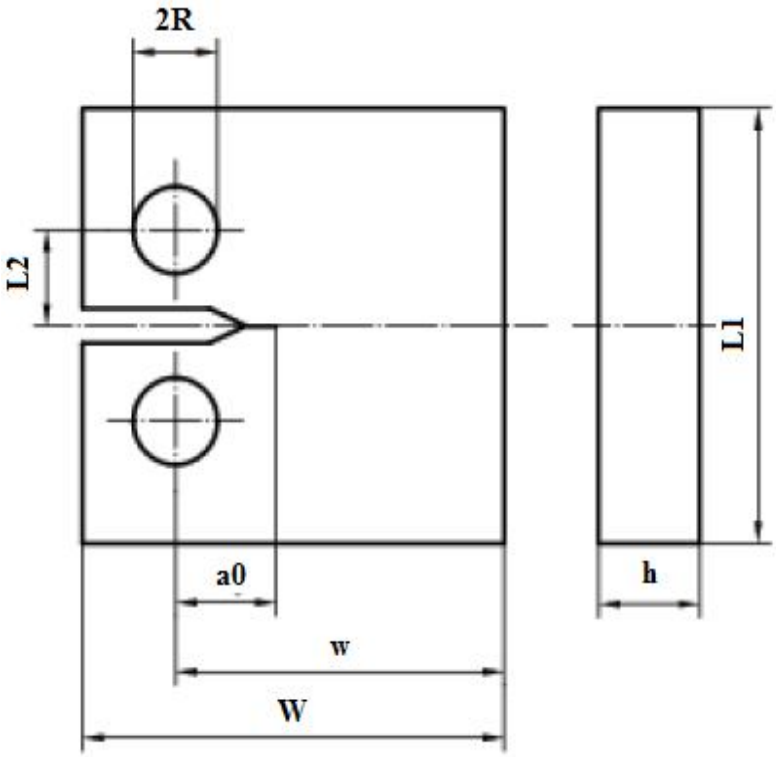

w/10 ≤ h ≤ w/2 (recommended)

W = 1,25w ± 0,01w

L1 = 1,2w ± 0,01w

L2 = 0,55w ± 0,005w

R = 0,125w ± 0,005w

a0 ≥ 0,2w

Figure 3.9: Standard dimensions of a Compact Test specimen according to ISO15850 [31]

3.3.3 Compact tension test: TDCB specimen

Despite the compact tension test using the classical CT specimens has been widely employed for testing the healing capability of modified matrices and has brought to several results, more recent studies (Brown [32]) doubted the reliability of such results due to the uncertainty in evaluating the pre-crack length after healing.

In fact, the definition of the healing efficiency as the ratio between two subsequent values of the fracture toughness K_{IC} is based on the connection of the latter with the applied force at fracture P_C and with a geometric factor basically depending on the ratio between the crack length *a* and the dimension *w* as defined in Fig.3.9 (Eq.3.5).

$$K_{IC} = \frac{2P_C}{b\sqrt{W}} f(a/w) \qquad (3.5)$$

The crack length of the virgin specimen can be measured without any problems, since it represents one of the design parameters, while it is greatly more difficult to evaluate it after

the healing process: in fact, depending on the percentage and the effectiveness of the healing agent, the two halves of the broken specimen can be completely or only partly joined together and to an extent that can be greater or smaller than the crack length of the virgin specimen. On the other hand, the simple assumption of a constant value of the crack length after the thermal mending can lead to extremely inaccurate results and wrong conclusions, involving an error which can be evaluated as follows:

$$\varepsilon = \frac{f(a_{virgin}/w) - f(a_{healed}/w)}{f(a_{healed}/w)} \times 100\% \qquad (3.6)$$

As a possible solution to this problem, Brown proposed the utilization of a Tapered Double Cantilever Beam (TDCB), which due to its peculiar geometry (Fig.3.10) presents an independence of the f function of Eq.3.5 from the ratio a / w (Fig.3.11). Consequently, the evaluation of the healing efficiency is much simplified, since there is no need to measure the new length of the crack. As shown with Eq.3.7, the new ratio turns out to be between the two limit values P_C of the force, when applied to the virgin and do the healed specimen.

$$\eta_{healing\ (K)} = \frac{K_{IC\ healed}}{K_{IC\ virgin}} = \frac{P_{C\ healed}\, f(a_{healed}/w)}{P_{C\ virgin}\, f(a_{virgin}/w)} = \frac{P_{C\ healed}}{P_{C\ virgin}} \qquad (3.7)$$

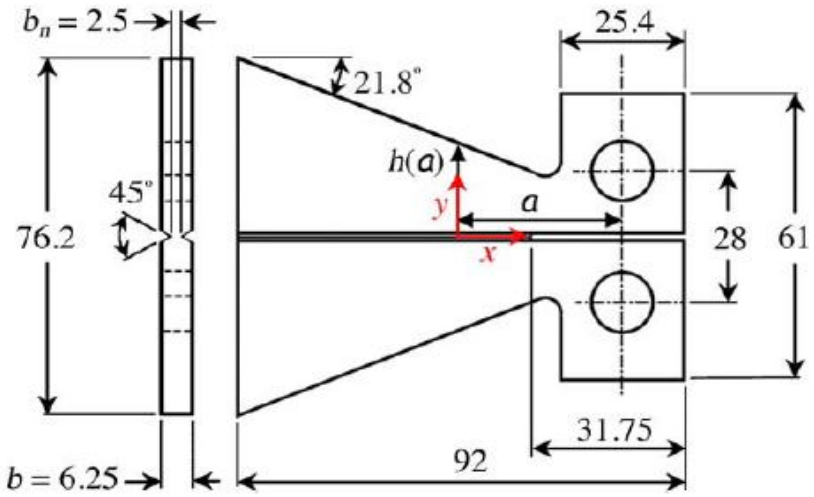

Figure 3.10: Geometry typical dimensions of a Tapered Double Cantilever Beam (TDCB) specimen as presented in [32].

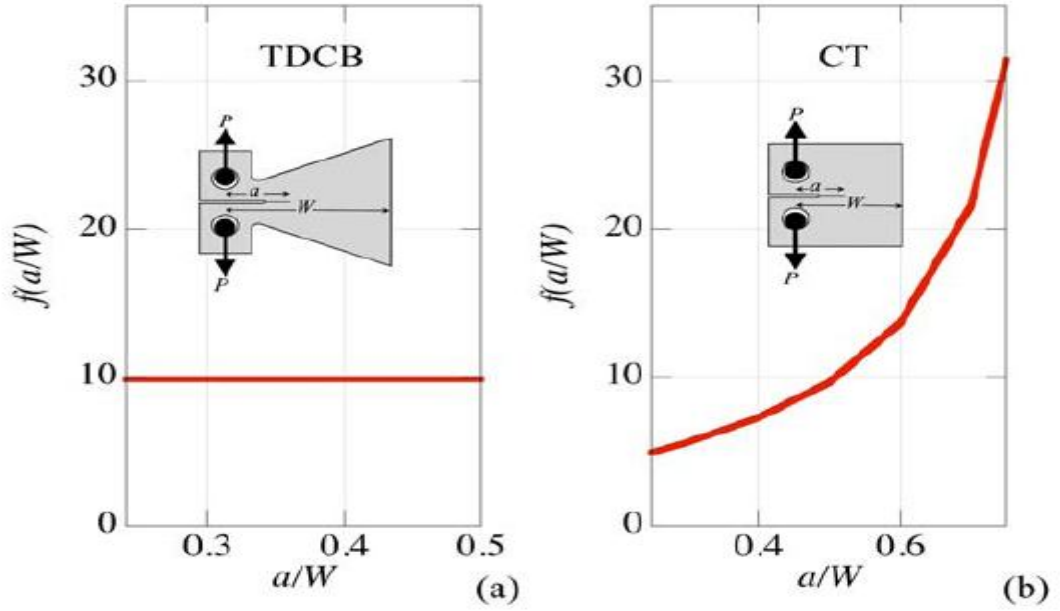

Figure 3.11: Relationship between the shape factor f and the ratio a / w (with the "a" dimension directly related with the crack length) for a Tapered Double Cantilever Beam specimen (a) and for a Compact Tension specimen (b) [32].

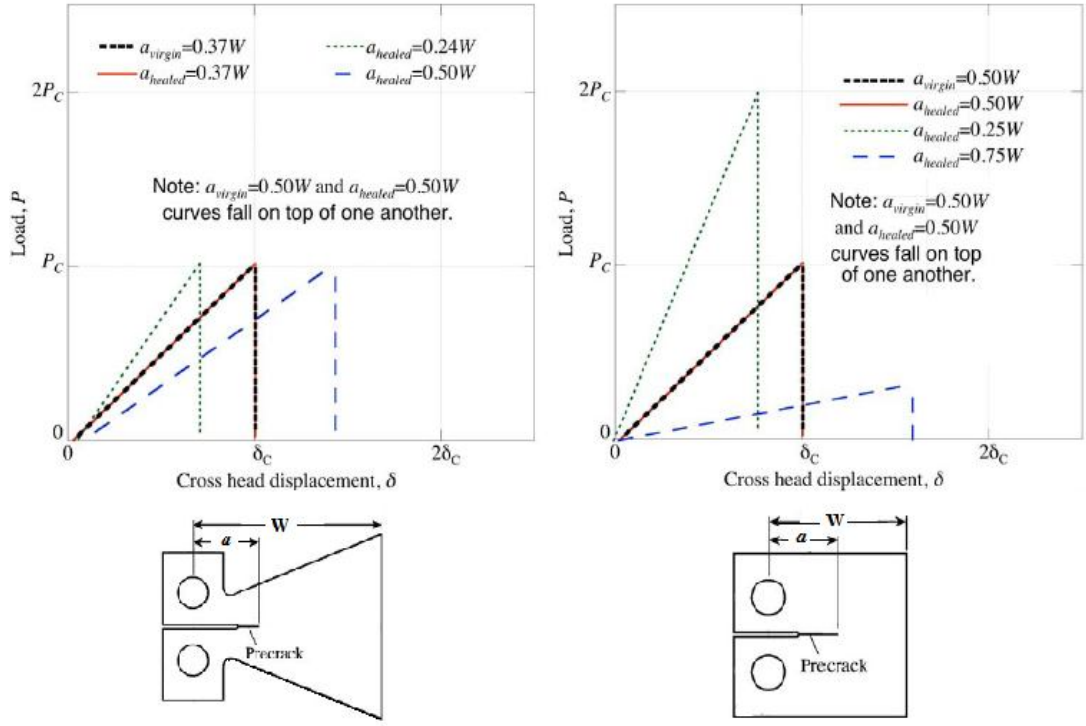

Figure 3.12: Variation of the value P_C of the peak load with the crack length for TDCB and CT specimens, compared to the value of the virgin specimen (bold dotted line). The first graph clearly shows the independence of the critical force P_C from the extent of the crack length a [32].

4 Surlyn experimentation

4.1 Introduction

"Surlyn®" is the commercial name chosen by DuPont™ for a random copolymer poly(ethylene-co-methacrylic acid) (EMAA) which has been partially neutralized with a Sodium, Zinc or Lithium cation (Fig. 4.1). The copolymer which is subjected to the neutralization process (trade name: "Nucrel®") has a 5.4 mol% of MA groups, disposed in the polymer chain with no specific order (hence the term "random"). According to the percentage of neutralized MA groups, several different kinds of Surlyn® are available (e.g. Surlyn® 8940 and Surlyn® 8920 are produced neutralizing respectively 30% and 60% of the methacrylic groups).

Being a ionomer, its healing action is based on the increase of mobility within the ionic aggregates, or clusters (see par. 3.2.3), by means of a heating process: ionomer chains are thus allowed to diffuse throughout the crack without altering the restricted mobility areas ("ion hopping").

Figure 4.1: Neutralization of the acid group of EMAA by means of Sodium [27].

4.2 Previous research

The ability of Surlyn® to self-heal has been investigated several times in last decade. In most of the performed experiments, Surlyn® pellets were used to create plate-shaped specimens to be tested to ballistic puncture.

Fall [27] studied the response to puncture of Nucrel® 925, Surlyn® 8920, Surlyn® 8940 and React-A-Seal®, in order to investigate the mechanism of self-healing. For the same purpose, these materials were also subject to Differential Scanning Calorimetry (DSC) and Dynamic Mechanical Analysis (DMA), to get information about the thermodynamic and viscoelastic properties.

The same classes of Surlyn® and two classes of Nucrel® (Nucrel® 925 and Nucrel® 960) has been further analysed by Kalista [28]. Material samples were created by means of a hot pressing process, which allows obtaining polymer films from the pelletized form of the material. Different damaging techniques were tested to study the influence of the involved energy on the velocity and efficiency of the healing action, while new ballistic tests were per-formed at different temperatures to state if the ionic content actually affects somehow the healing efficiency. The first set of experiments showed how the self-healing can autonomously happen only when the damaging action involves friction: in fact, healing was observed after ballistic puncture and sawing, but not after simple cutting or needle puncture. In addition, the ballistic tests highlighted the importance of the elastic response of the material, since, when the elastic properties were decreased by a higher temperature, the healing efficiency was greatly lower. Finally, the neutralization of the ionic groups has been proven to be unessential for the patching of the projectile hole, for it occurs in the unneutralized material (Nucrel®) as well.

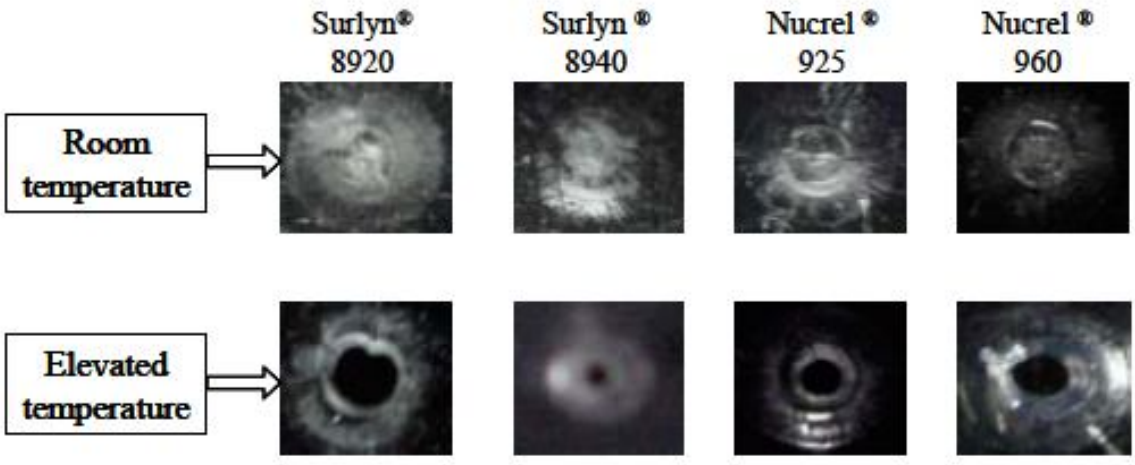

Figure 4.2: Differences in the self-healing action at different temperatures [28].

Further researches [29,30] were focused on better understanding the concurrent action of elastic and viscous responses. The possibility of repeated healing was also inspected and confirmed, demonstrating that the mending ability is intrinsic in the ionomeric chemical structure.

4.3 Mixing tests and results

Most of the recent researches have been carried out in order to investigate the properties and the behaviour of the ionomeric material itself, basically not considering any possible application in composite matrices. Thus, the former purpose of this work has been to examine the possibility of creating a matrix with self-healing properties, using a blend of ionomers and epoxy resin. The material chosen for the purpose is Surlyn® 8940 (30% of the methacrylic groups is neutralized), available in pelletized form.

4.3.1 First test

Since the solubility of Surlyn® in epoxy resin had yet to be proved, the first mixing test was performed without paying particular attention to the percentage of healing agent used: the optimal amount would be object of further research and tests. For what the mixing operation is concerned, it was done according to the one recommended by InChem for phenoxy pellets. According to this, some grains of Surlyn® were added to the epoxy resin (Huntsman Araldite LY1556), which had been previously heated to 60°C by means of an electrically heated plate, then the temperature of the mixture was slowly increased. Due to a heavy uncertainty in setting the heating device, some difficulties were encountered in thermal measurements. The increasing of temperature was followed using an infrared thermometer from an approximated distance of 30 cm. However, exact values are not essential for the purpose of the test performed. Moreover, because of the small quantities utilized for the test, the use of an automatic stirrer was not possible, hence the mixing operation has been brought on manually.

According to the Surlyn® data sheet [33], the melting temperature is 94 °C, while the nominal processing temperature ranges from 185 to 285 °C. Though, no signs of dissolution were detected once surpassed the threshold of 94 °C. The temperature was hence increased gradually, finally reaching the value of 195 °C (higher values have not been set, since the degradation temperature of Araldite is reported to be of 200 °C [34]).

This status was kept constant for two hours, yet the ionomer grains were still clearly visible in the mixture, moreover maintaining a solid structure (Fig.4.3).

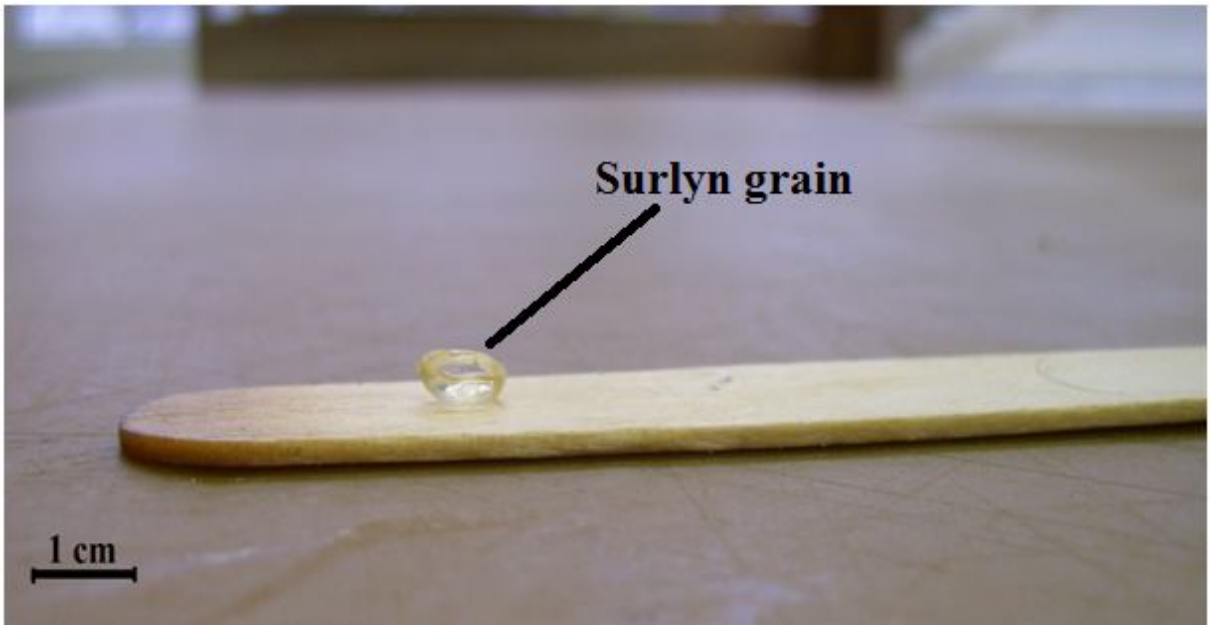

Figure 4.3: A Surlyn pellet as it appears after the first mixing test. Melting and dissolution are clearly far from being achieved.

4.3.2 Second test

DSC analysis

Before performing new tests, Surlyn® was subject to Differential Scanning Calorimetry (DSC) to check any dissimilarity between the effective melting temperature of the available material and his nominal value, reported in its data sheet.

This kind of test allows to obtain the temperature at which the phase transition occurs, by comparing the heat needed to maintain the analysed material and a reference material at the same temperature. Hence, since the melting of the solid specimen involves an endothermic reaction, this is highlighted by a greater heat flow to the analysed specimen.

Fig.4.4 shows the results obtained for Surlyn® 8940. In the reported chart, the peaks represent the fusion of the material, which occurs for the greater part at 91.8 °C and for the remaining part at 102.5 °C. Thus, nothing but a slight difference is noticed between the nominal and the observed values.

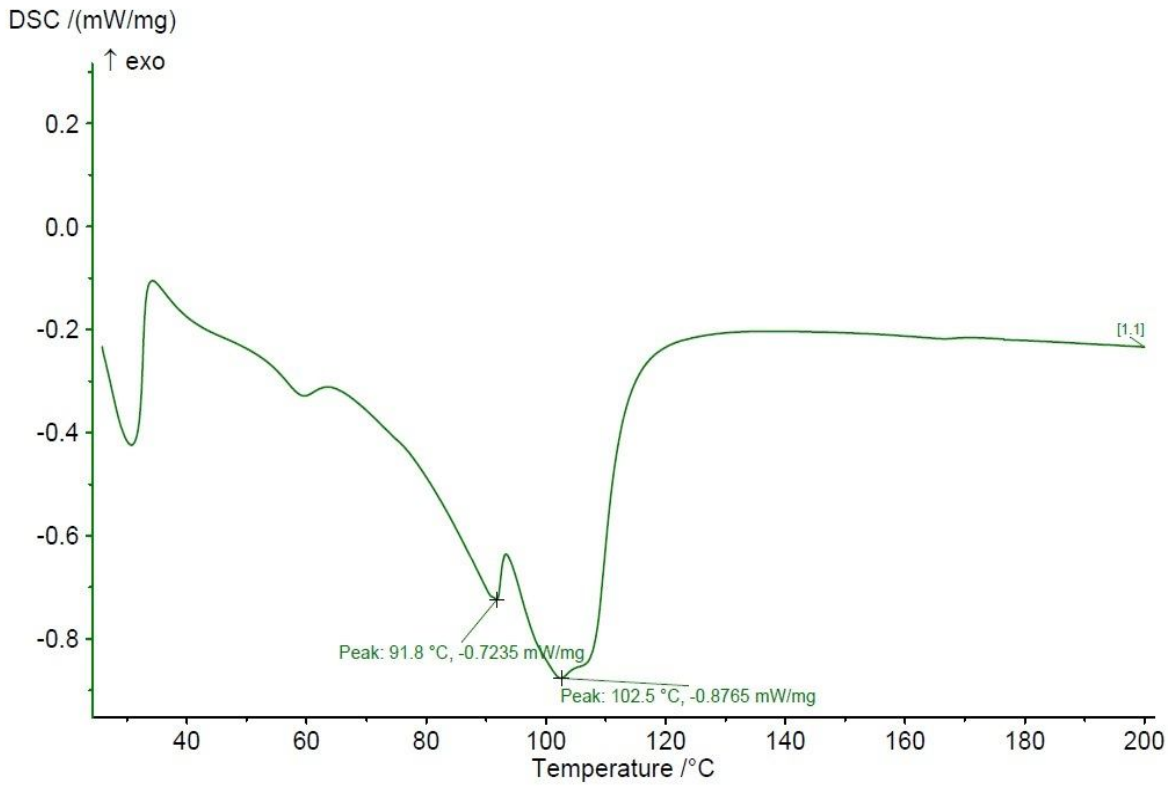

Figure 4.4: Result of DSC test for Surlyn© 8940. The two peaks represent a first partial melting at 91.8 °C and the completion of the phase transition at 102.5 °C.

Crushing the pellets

After the unsatisfying results obtained in the first test, it was thought that the failure of the mixing operation could be partially or totally due to the granular shape of the healing agent: in fact, the pelletized form could enhance an intrinsic difficulty in solving the Surlyn® in the epoxy resin, making the process very arduous or even impossible.

According to this belief, the subsequent test has been focused on reducing the size of the grains by pulverize them with a centrifugal crushing machine. Since a mechanical action on the unaltered pellets would bring to nothing more than a deformation in shape, the material has been first embrittled by means of liquid nitrogen. Nevertheless, the production of a powder has been time consuming and far from being satisfactory. In fact, the machine could not be loaded with a big quantity of grains without incurring failure and blocking, and moreover the dimension of grains in the so obtained powder, though reduced, could not present a significant difference from the unaltered material. A second treatment with the crushing ma-

chine, if on one hand could have led to a finer product, on the other hand would have brought a further increase in an already long processing time and hence was not performed.

Yet, a small amount of crushed grains has then been mixed with epoxy resin and the procedure reported for the first mixing test was replicated, in order to detect any solubility amelioration. As a heating device, a microwave oven was used, in order to grant a more uniform heat supply. Before pouring the grains, the resin has been heated at 60 °C, then the mixture has been slowly brought to 135 °C and periodically manually stirred.

Although a loss in the grains hardness could be detected, since their shape could be altered by means of mechanical action, yet neither complete melting nor solving in the Araldite were observed.

4.3.3 Third test

Since the solubility of Surlyn in epoxy resin has proved to be very poor, an attempt of creating an homogeneous blend was made using a phenoxy resin as intermediate agent. Phenoxies are thermoplastic resins resulting from the reaction of epichlorohydrin with bisphenol A and have the interesting characteristic of a good solubility in epoxy. In fact, while a successful mixing with an ionomeric additive is still uncertain, the achievement of phenoxy-epoxy solutions are reported in literature to be feasible and used [20].

The object of this last test was the solid form of a resin obtained by previous internal researches, in which Surlyn has been added to a mix of phenoxy resin and carbon nanotubes by means of a hot pressing process (Fig.4.5.a).

Following a procedure similar to what presented in the previous tests, a small amount of the solid material was turned into fragments and added to the Araldite, performing then both manual stirring and a slow and continuous increase of temperature to finally reach the value of 135 °C.

As expected, the phenoxy resin presented no difficulties in melting at the set temperature, homogeneously mixing with the epoxy. On the other hand, the ionomeric fraction was observed to separate in several aggregates without exhibiting any clear phase transition. As shown in Fig. 4.5.b, this behaviour is highlighted by the carbon nanotubes mixed with Surlyn. Further stirring brought no amelioration in the final results, even when performed automatically, nor a rising of the temperature until the degradation threshold of the epoxy could produce any dissolution.

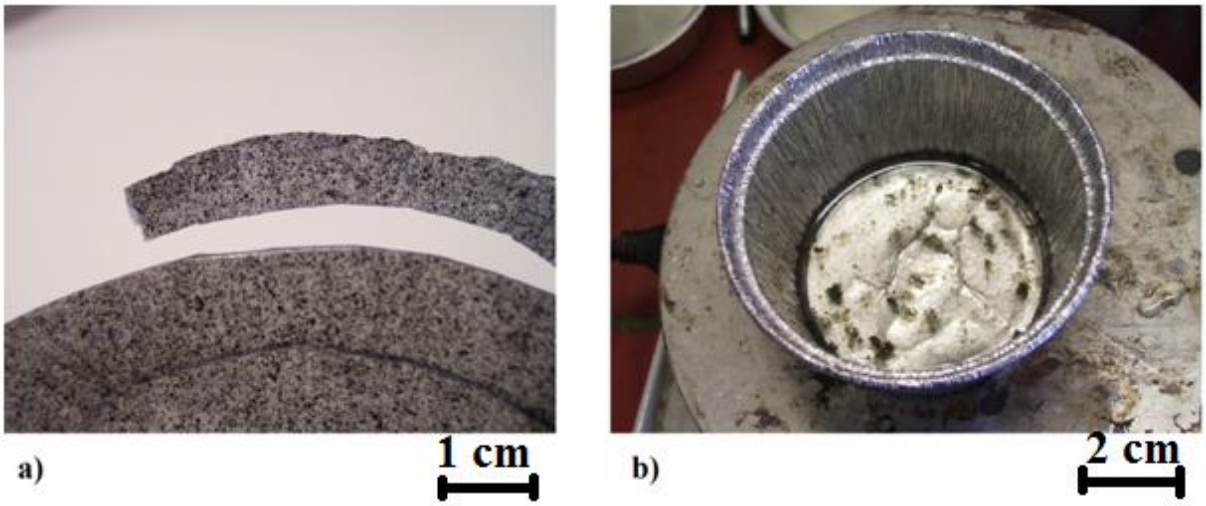

Figure 4.5: Mixing test using phenoxy: a) shows the solid form of the mixture of phenoxy resin with Surlyn 8940 and carbon nanotubes, while b) represents the blending as it appears after the mixing process. The separation of the Surlyn fraction is clearly visible in the aggregations of nanotubes, which are partially trapped in the material.

4.4 Conclusions

The failure in reaching the desired outcomes in all the performed tests clearly highlighted the difficulties in creating a self-healing resin from a homogeneous mixture of epoxy resin an Surlyn 8940.

This behaviour is due to the attempt of simply melting the pelletized form of the healing agent without performing any heavy mechanical action and to the intrinsically poor solubility of Surlyn itself. In fact, no previous mixing tests have been found in literature, since the healing action was analysed considering thin films or plates made of sheer material [12, 27, 28, 29, 30]; moreover, a common feature in the mentioned experiments was the use of the compression moulding process to obtain specimens from the Surlyn pellets (temperatures and pressures vary depending on the authors).

To date, in the light of the experiments reported above, the use of Surlyn for the creation of a self-healing thermosetting matrix is yet to be achieved. For the goal of this research, hypothesizing an analogous behaviour for all ionomers, it was decided to focus the further studies on healing agents acting with a different mechanism.

5 Thermoplastic additive experimentation

5.1 Introduction

After proving the ineffectiveness of blending Surlyn 8940 with epoxy resin, there was the need of finding another material which could successfully act as healing agent for a matrix. Assuming a similar behaviour for all ionomers, new attention was paid for other kinds of healing mechanisms, such as micro-containers or thermoplastic additives. Considering advantages and drawbacks of each possibility (see par.3) for an eventual employment in composite material, the one of a blend with thermoplastic polymers has been thought to be the most suitable for the purpose.

This approach (see par.3.2.2) is based on the creation of a blend in which a substrate of thermo-setting resin is added with a set percentage of a chosen thermoplastic polymer representing the healing agent. Upon heating, the diffusion of the latter in the thermosetting matrix is enhanced, thus allowing the bridging of cracks and subsequent healing (Fig.5.1). However, to properly perform the process there is the necessity for the crack to be closed, with a good alignment of the crack edges, and therefore the component subjected to healing must be free from any tensile force. Moreover, the presence of a compressing force while supplying heat could positively influence the recovery of the specimen.

On the other hand, the modification of the matrix with a lower-resistance material could bring to a decrease of the mechanical properties in a measure depending on the quantity of dissolved additive. Therefore, the percentage of healing agent must be accurately set by pondering the above exposed advantages and drawbacks of this solution.

In the following chapters, the choice and testing of a thermoplastic-thermosetting blend is described, with particular attention to the parameters which, positively or negatively, affect its properties and its recovery.

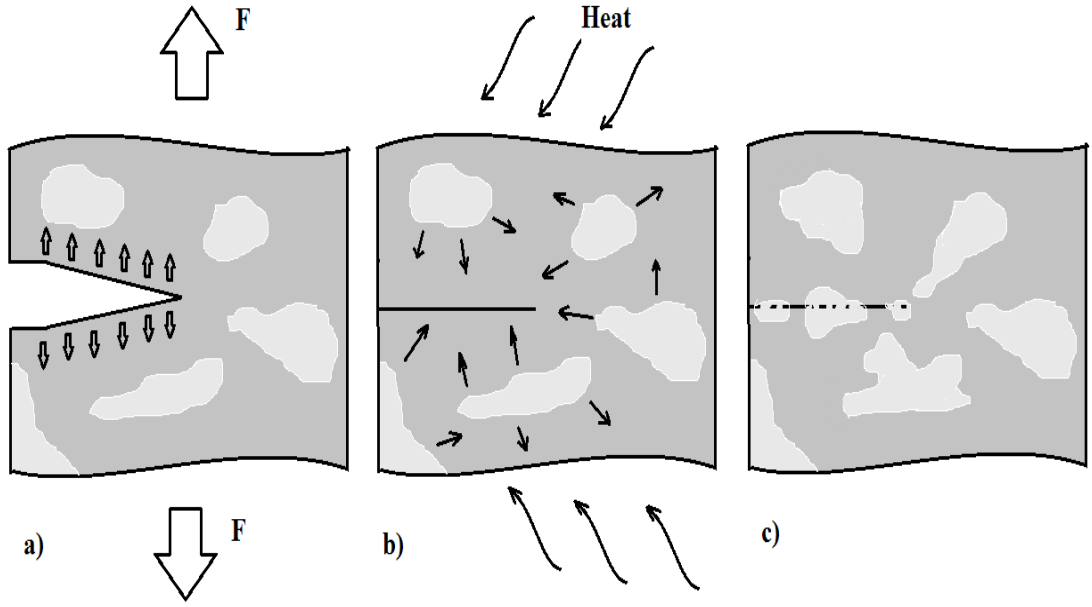

Figure 5.1: A schematic representation of the healing process based on the dissolution of a thermoplastic resin (brighter spots) within the thermosetting matrix. The distribution in spots has only an explanatory reason, since the additive has to be thought to as uniformly dissolved in the thermosetting resin. a) Action of a tensile stress which results in the opening of the crack; b) Heating of the unloaded material and diffusion of the healing agent; c) Bridging of the closed crack during the cooling time.

5.2 Materials used

5.2.1 Epoxy resins

For this series of experiments, Araldite LY 1556 produced by Huntsman has been employed (Fig.5.2.a), for which the decomposition is reported to occur at over 200 °C and which is thus suitable for a wide range of processing temperatures [34].

5.2.2 Accelerator

The selected accelerator for the used resin system is Accelerator 1573 (Fig. 5.2.b), as reported in Huntsman's Data Sheet [35].

5.2.3 Hardeners

The system used in this work is characterized by two different curing agents, Aradur 1571 and Hardener XB 3403 (respectively shown in Fig. 5.2.c and 5.2.d). According to Huntsman's technical data sheet, three different systems can be produced (Tab.5.1).

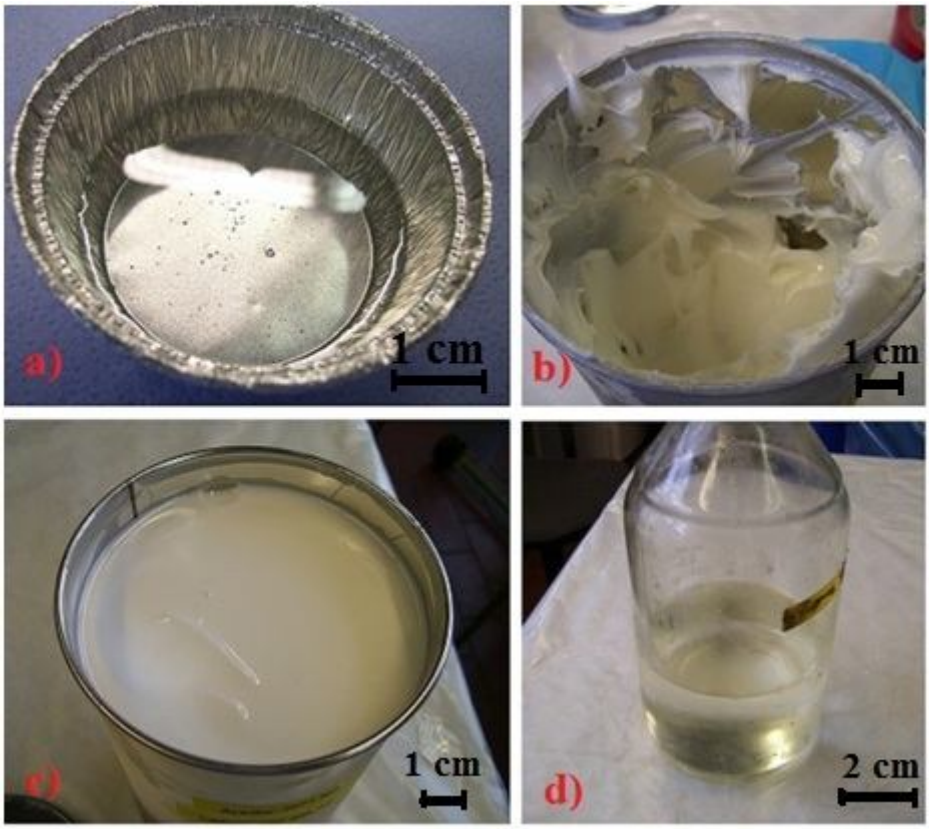

Figure 5.2: Components used for the production of the unmodified epoxy resin: a) Araldite LY 1556; b) Accelerator 1573; c) Aradur 1571; d) Hardener XB 3403.

Table 5.1: Mix ratio for three different resin systems, as reported by Huntsman's data sheet.

Components, parts per weight	System 1	System 2	System 3
Araldite LY 1556	100	100	100
Aradur 1571	23	23	23
Accelerator 1573	3	5	7
Hardener XB 3403	12	12	12

5.2.4 Healing agent

After an overview on the different possibilities, it was decided to use a phenoxy resin as healing additive for the epoxy system. This material is a linear thermoplastic polymer which is obtained from the reaction of epichlorohydrin with bisphenol A and has been chosen for its good solubility in epoxy resin, due to a great similarity in the chemical structures. This feature

has made phenoxy resins very suitable for producing soluble yarns, which are widely used to avoid the distortion of reinforcing fibres of composites during the resin infusion process.

The phenoxy used in this work is the InChem's PKHB resin, which presents a very low molecular weight and is available in pelletized form (Fig. 5.3).

Figure 5.3: Pellets of phenoxy resin (PKHB) [36].

5.3 Mixing of Araldite LY 1556 and PKHB resin

5.3.1 First mixing test

Though many studies reported the good solubility of phenoxy resins in epoxy, after the bad results obtained with Surlyn a preliminary solubility test was thought to be useful for evaluating the time consumption of the process and for detecting possible complications. A first mixture was thus prepared adding some PKHB pellets to the Araldite and performing a manual stirring. For the purpose of this first experiment, an accurate weighing of the components was not necessary, so that the quantity of pellets added to the resin was set randomly. The adopted procedure was the one provided by InChem for incorporating phenoxy pellets of any grade into liquid epoxy resins: the temperature of the epoxy was increased by means of a heating plate and the sifting of the phenoxy pellets was performed when the resin reached the value of 60 °C. The final temperature has been set to be 140 °C and the manual stirring was brought on for all the duration of the process.

Because of the small quantities which had been employed, a complete dissolution of the grains could be visually determined after a shorter time than the 2 or 3 hours reported in the InChem paper (about 90 minutes). The heat supply was then turned off and air cooling was allowed.

Though the positive results could allow the subsequent experimentation with a more accurate weighing of the components, the tendency for the pellets to aggregate and stick together

was observed, thus suggesting the possibility of further reducing the process times when this behaviour could be avoided.

5.3.2 Blend composition

Before starting new tests, it was necessary to set a proper weight percentage for the components of the blend. Since the first experiments would have focused on determining the effectiveness of the healing action, a high fraction of phenoxy was thought to be preferable for better highlighting this phenomenon. On the other hand, due to the higher viscosity of thermoplastic resins, a too high concentration would have brought difficulties while processing. For these reasons, the quantity of phenoxy pellets was set to be 10 wt% of the epoxy resin (resulting in a weight percentage of approximately 9,1 wt% in the blend). It is essential to notice that adding a thermoplastic component to a thermosetting resin has a detrimental effect on its mechanical properties. Though, their variation with the percentage of healing agent has not been investigated in this work and could thus be object of further research.

5.3.3 Mechanical stirring test

After the successful results of the first mixing test, a new series of experiments was started in order to find a way to produce a good quantity of modified resin in a relatively short time, since a manual stirring of a large amount of material would be too time consuming.

According to the fact that the aggregation of the pellets and their sticking to the walls of the vessel could be avoided with a faster and more continuous mixing, a mechanical mixer mounted on a rotating spindle was employed for blending a trial quantity of 100gr. of epoxy with 10gr. of phenoxy. The mixing tool, with a head diameter equal to about 90 % of the diameter of the vessel, was set to a rotating speed of 200 rpm and plunged in the epoxy once the temperature of 60 °C was reached, then the phenoxy grains were added to the resin and the temperature was slowly brought to 140 °C. In spite of the lower viscosity of the resin resulting from the increasing temperature, nevertheless a clamping device has been necessary to secure the vessel to the heating plate and contrast the centrifugal forces resulting from the stirring action.

The results showed that the unwanted tendency of the pellets to stick together could not be avoided by the mechanical stirrer. In fact, a considerable part of the material was found attached to the bottom of the vessel and to the mixing blades even after a time way longer than

the 90 minutes needed during the first phase of the experimentation (see par. 5.3.1) and for this reason the accuracy of the previously set weight proportions was greatly affected. On the other hand, due to the small clearance between the blade edges and the walls of the vessel, a manual intervention for detaching the grains could not be performed without interrupting the mixing operation.

Hence, as it was performed, this process could not be suitable for the purpose and other methods had to be investigated.

5.3.4 Mixing rolls

Another possible alternative for the production of a homogeneous blend was represented by the mixing rolls usually employed for embed carbon nanotubes in epoxy matrices. The machine and its action are schematically represented in Fig.5.4: the blend is obtained by passing the firstly unmixed components through a row of heated rolls with set clearances and speed.

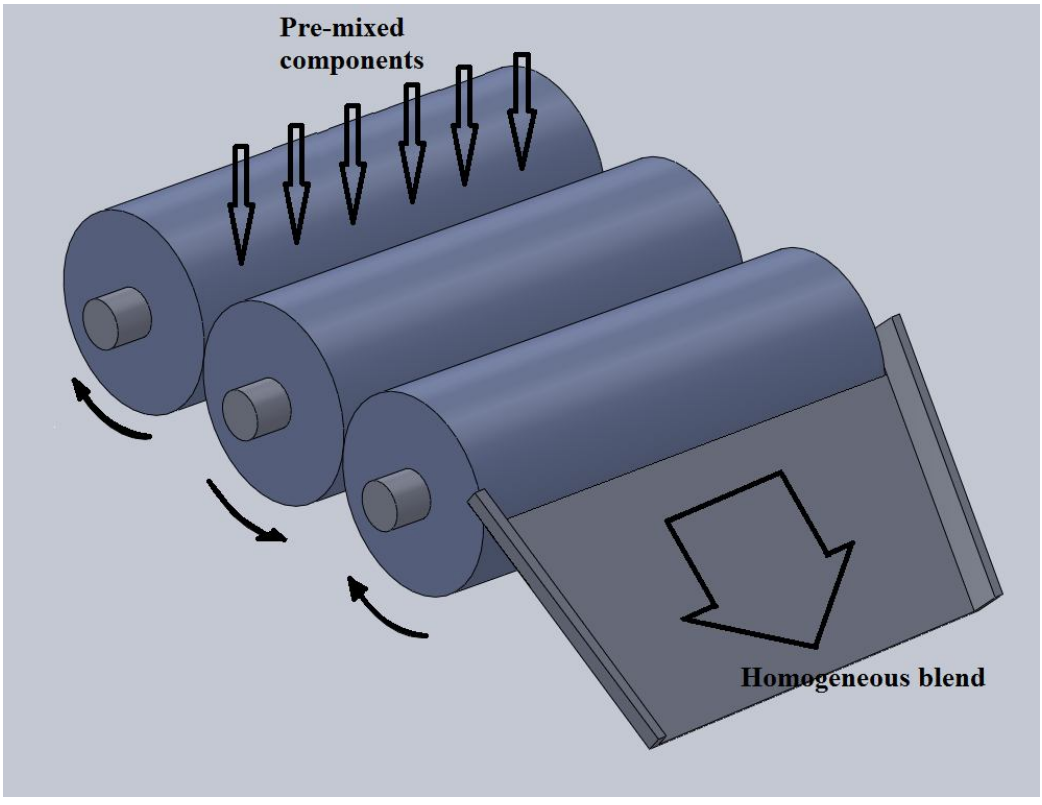

Figure 5.4: Schematic representation of the mixing operation by means of heated rotating rolls.

While the process is normally brought on to achieve an uniform distribution of the CNTs in the matrix, in the examined case the pressure and the heat supplied by the rolls must succeed in melting the phenoxy grains and properly dissolve them throughout the epoxy resin.

The process was brought on by performing three passages of the blend through the rolls, in order to obtain a finer result. For all of the three iterations the velocity has been set to 300 rpm, while the clearances between the rolls has been changed for the third passage: for the first two times, the first clearance has been set to 40 μm and the second to 14 μm, while for the third the gaps have been reduced to 13 μm and 5 μm respectively. For the temperature, a ramp input was chosen to finally reach the value of 190 °C. The components have been mixed following the previously chosen, with an amount of PKHB pellets fixed to 10 wt% of the quantity of epoxy. For each passage through the rolls, the resulting compound has been collected in a vessel and reintroduced in the machine.

The solution adopted proved to be effective for what the mixing is concerned, as the phenoxy pellets resulted to be melted and homogeneously dissolved within the epoxy resin. Although, this process could not be considered fully effective since a too large quantity of mixture was lost when passing through the rolls, probably due to a bad adhesion to the surfaces. Thus, the operation with the mixing rolls had to be abandoned as not suitable for a larger scale production.

5.3.5 Magnetic stirrer

The third method investigated for mixing the components finally brought satisfactory results and was thus adopted for producing the amount of compound subsequently used for the research. The mixing operation was performed by means of a magnet plunged in the resin mixture and subjected to a rotational magnetic field.

For the purpose, a magnetic stirring machine was adopted, in which the temperature of the heating plate and the rotational speed of the magnetic field can be regulated by the respective knobs. The complete experimental apparatus can be seen in Fig.5.5: a bath of oil was employed to convey a uniform heat to the resin mixture, whose container has been clamped to a supporting rod. Two bar-like magnets ensure respectively the rotation of the oil and the mixing of the resin (it is thus obviously essential to properly adjust the clamping of the resin vessel, in order to allow the free movement of the magnet). Differently from what reported for the mechanical stirring operation (see par. 3.3.3), this layout offers the advantage of a better

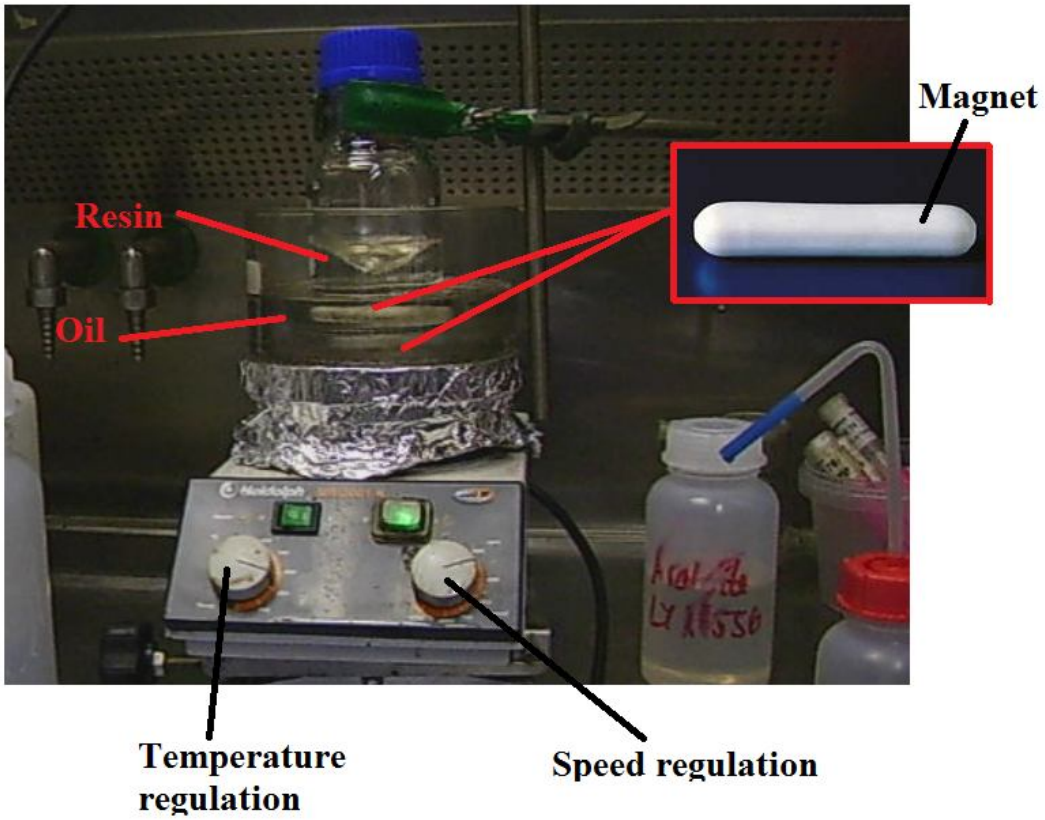

Figure 5.5 : Experimental apparatus for the magnetic stirring operation.

accessibility to the mixing area, in case a manual intervention to avoid the sticking of the grains is needed.

As reported in the sheet provided by InChem, the first step of the procedure has been to slowly increase the temperature of the epoxy resin before adding the PKHB pellets. The rotational speed of the magnetic field was set to approximately 500 rpm. The initial contrast to the motion resulting from the resin viscosity was automatically solved with the increase in temperature, while any possible irregularity in the movement of the magnets, due to reciprocal magnetic interference, could be avoided by a very slow increase of the velocity. Once the temperature of 60 °C was reached, the phenoxy grains were added little by little using a funnel and subsequently more heat was supplied to finally reach 140 °C.

This solution and the gradual adding of the pellets allowed a good stirring of the compound, without any noticeable sticking phenomenon. A very good dissolution of the PKHB has been detected after 40 minutes from the beginning of the operation, a lapse of time far shorter than what could be obtained with manual stirring. The process has then been considered the most suitable for producing the quantity of modified resin needed for the preparation of the Compact Tension specimens.

A quantity of 440 gr. of mixture was then produced with four subsequent stirring operations, each of which processing 110 gr. of product.

5.4 Production of the CT specimens

After obtaining an acceptable amount of thermoplastic-modified epoxy resin, the procedure for the production of Compact Tension specimen was started. The first step has been mixing the obtained resin system to the other components presented in par.5.2, in order to finally achieve the polymerization and the hardening of the matrix in a proper mould. After curing, the resulting resin plates have been cut according to the set of dimensions determined for the specimens. For comparison purpose, a set of specimens was prepared using a resin system with unmodified epoxy resin.

It should be noted that the most challenging problem encountered has been the enhanced viscosity of the resin, due to the addition with a thermoplastic component, which necessarily brought to some modifications in the procedure and in the shape of the specimens.

5.4.1 Preparation and curing of resin plates

For setting the quantities for each element, the procedure provided by Huntsman was followed, considering for the new resin system the percentage reported for the unmodified Araldite LY 1556 (system n.2). Thus, the composition of the system was set as reported in Table 5.2. The quantities adopted for the first plate have been slightly increased for the following plates to better fill the mould, yet maintaining unaltered the ratios between the components.

Table 5.2: Quantities for the resin system as reported on Huntsman's data sheet and as adopted for the first plate of modified matrix.

Components	Parts per weight (Huntsman, system n.2)	Quantity 1st Plate [gr.]
Araldite LY 1556 + PKHB	100	118.98
Aradur 1571	23	27.36
Accelerator 1573	5	5.94
Hardener XB 3403	12	14.28

For the first trial, all the components, kept in different vessels, have been put in a vacuum chamber and processed until the complete evacuation of the air inclusions. For better results, all the elements had been previously heated in oven for 10 minutes at 35 °C, in order to reduce the viscosity. After no more bubbles were observed to form, the components have been taken out to be mixed together, having care to perform a very slow stirring and thus to reduce as possible the amount of air newly trapped within the blend. Firstly, as reported in the data sheet, Aradur and Accelerator have been mixed together, then they have been added to Araldite together with the Hardener, performing a slow stirring to obtain an homogeneous paste. In a comparison with the unmodified epoxy, a markedly higher viscosity was found to characterize the new system. A second phase in the vacuum chamber, brought on while stirring the blend by means of the incorporated spindle, further highlighted this aspect, since the evacuation of the trapped gases could not be completely fulfilled. Being 40 minutes the approximated time needed for the hardening to begin, the degassing process had to be interrupted to avoid the cross-linking within the vessel.

According to the dimensions chosen for the Compact Tension specimens (see following chapter) a mould with a thickness of 7 mm was used for the preparation of the plates. A schematic representation is given in Fig.5.6: for a better ejection of the resin plate once the solidification has occurred, the mould is composed by two halves which are clamped together by means of a set of screws. A Teflon layer prevents the sticking of the material to the bottom while solidifying and in addition a release agent was passed twice on all the surfaces of the mould which would be in contact with the molten resin, i.e. the upper surface of the lower half and the base and internal walls of the upper half. The second layer of release agent was

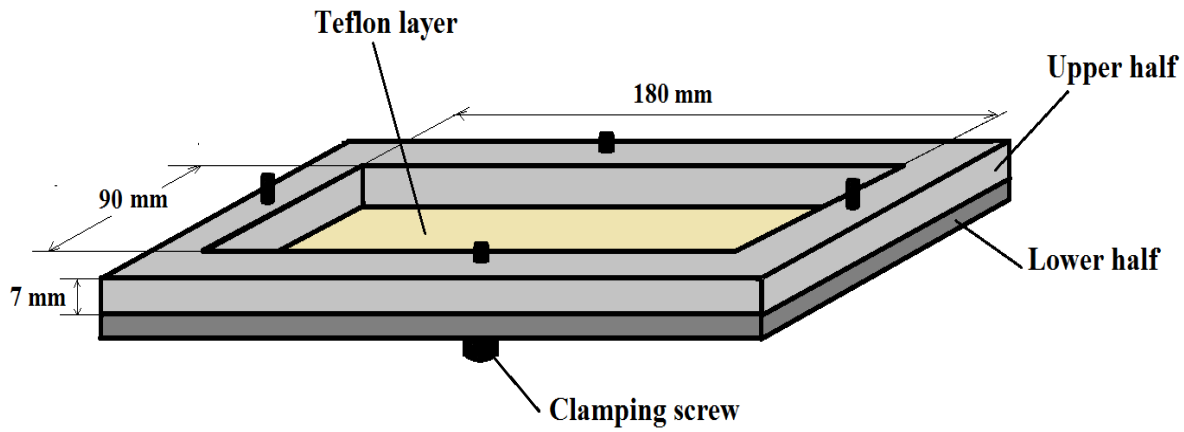

Figure 5.6: Scheme of the mould used to prepare the resin plates.

applied after the complete drying of the first one and the whole operation had to be completed at least ten minutes before filling the mould, in order to allow the second layer to solidify.

The subsequent phase of pouring the resin highlighted the problems related to an enhanced viscosity in the modified matrix, since the natural flow of the molten material would bring to an incomplete filling of the mould and a manual intervention has been hence necessary to provide a satisfactory distribution in the cavity. Nevertheless, the flowing difficulty brought to the impossibility of obtaining a constant thickness in the poured layer, which could have been better achieved with a less viscous fluid as unmodified epoxy. Moreover, after distributing the material a noticeable quantity of air inclusions was still visible on the layer's surface, probably due to the incomplete degassing action performed in the vacuum chamber and to the necessity of spreading the molten resin by hand. Although, this problem, yet not cancelled, could be reduced with the subsequent curing stage.

After the pouring, the so-called "B-staging" was performed, in which the material was left for 48 hours at room temperature. Being a partial flow of the molten resin still possible in this phase, it was essential to verify the horizontality of the surface on which the mould had been placed. Once the B-staging has been completed, the plate was put into the oven for the final part of the curing process. Before the placement of the mould, the oven had been pre-heated to reach the temperature of 60 °C. Then, the temperature has been gradually risen with an increment of 20 °C every 10 minutes, to finally reach the value of 120 °C. This temperature was maintained for two hours, as indicated in the Huntsman's data sheet, then the mould was extracted to allow air cooling. The previous applying of two layers of release agent permitted an easy removal of the plate by simply acting on the clamping screws and applying a slight pressure on the upper half of the mould.

The modified resin as it resulted after the final processing stage is presented in Fig.5.7.a, in which the plate has already been cut in two halves: the comparison with a plate made of unmodified epoxy and obtained following the same processing parameters (Fig.5.7.b) clearly shows how the self-healing matrix was affected with a large amount of gas inclusions, which heavily compromised the integrity of the material and its effective usefulness for producing defect-free specimens. Moreover, even with a slight improvement probably obtained during a redistribution of the material during the B-staging, yet a uniform thickness of the plate could not be achieved.

A change in the processing parameters had thus to be done in order to limit this feature in the other plates. As hinted at the beginning of the chapter, the quantity of each component

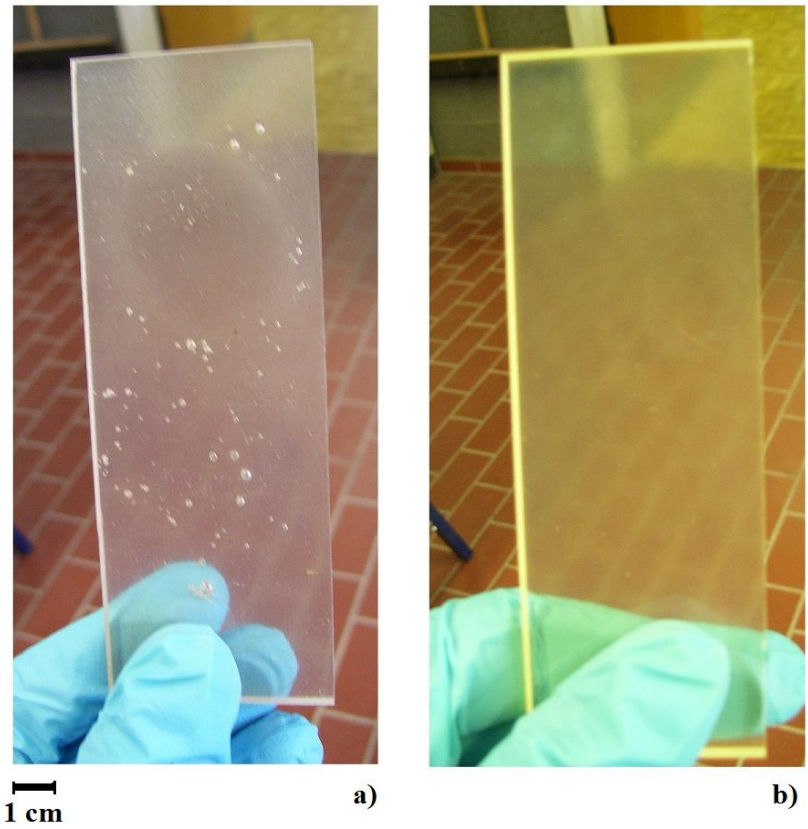

Figure 5.7: Comparison between a plate made of self-healing resin (a) and a plate of unmodified epoxy (b) produced with the same process. The better quality of the second one is clearly visible.

was increased, obviously without altering the weight ratios, in order to face the problem of dimensional irregularities by rising the overall thickness of the resulting plate. For what the gas inclusions are concerned, a higher temperature could temporarily reduce the viscosity of the material, thus allowing a more successful degassing operation. Being not feasible to heat the blend inside the vacuum chamber, even to avoid an early polymerization, a rise in temperature was performed during the heating of the separate components, changing from the initial 35 °C to a value of 70 °C , while the time duration was brought to 20 minutes.

The adopted changes proved to be satisfyingly effective for ameliorating the final quality of the produced plates: although no difference could be detected in the material viscosity during the pouring in the mould, in fact, more time was needed to reach the room temperature, thus allowing a better evacuation of the trapped gas. In addition, the greater amount of material brought a greater part of the plate to reach the limit value chosen for the specimens' thickness.

5.4.2 Design and preparation of the specimens

After a satisfactory amount of resin was produced, the process of cutting the plates into the desired shapes has been brought on. It has to be noticed that, even if the overall geometry of the employed elements has been defined following the guidelines for traditional Compact Tension specimens (see Fig.3.9), some features had to be added or modified to overcome the problems encountered in the previous phase of production of the resin, or to better achieve the specific purposes of the tests to be performed.

The first problem to face has been the determination of a proper thickness for the specimens. In fact, if on one hand the condition of plane strain essential to grant the reliability of the test could not be achieved under a specific value of the thickness itself, on the other hand there was the need to eliminate from the available plates the irregularity of such dimensional parameter. Moreover, the outer layer of the plates had necessarily to be removed in a grade depending on the depth of the air inclusions, to allow the production of defect-free specimens. Thus, it was thought that a thickness of 5 mm could be a good compromise between the concurring design needs and, being this the geometrical feature which mostly was influenced by the previous operations, every other dimension was set as its function.

In addition to this, a new modification was made according to the peculiar need to newly use the specimens after the first breakage. As previously hinted in the Introduction, a proper healing action on the broken specimen can only occur if the crack is closed and the two halves are brought to a perfect coincidence, and for this reason it was thought that a complete separation should be avoided. One solution to this aspect has been proposed by Jones et al. [21] and consists in drilling a hole by the plane of symmetry of the specimen, which ideally represents the path of a growing crack. With this device, the failure of the specimen is localized to the portion of material between the pre-cracked notch and the hole, which blocks any further damage propagation, and the realignment of the parts is theoretically granted once the tensile load is released. This solution was thus adopted for its simplicity and reported effectiveness and a 6 mm hole has been added to the geometrical features of the considered specimens. For the same purpose of a better realignment after the failure of the specimen, the length of the notch was slightly reduced, in order to allow a more central position of the hole yet maintaining an acceptable area of material for the propagation of the crack. The complete set of dimensions used for the construction of the specimens is reported in Fig.5.8. It has to be noticed that the dimension of the clamping holes has been decided on the base of the loading pins available for the testing machine.

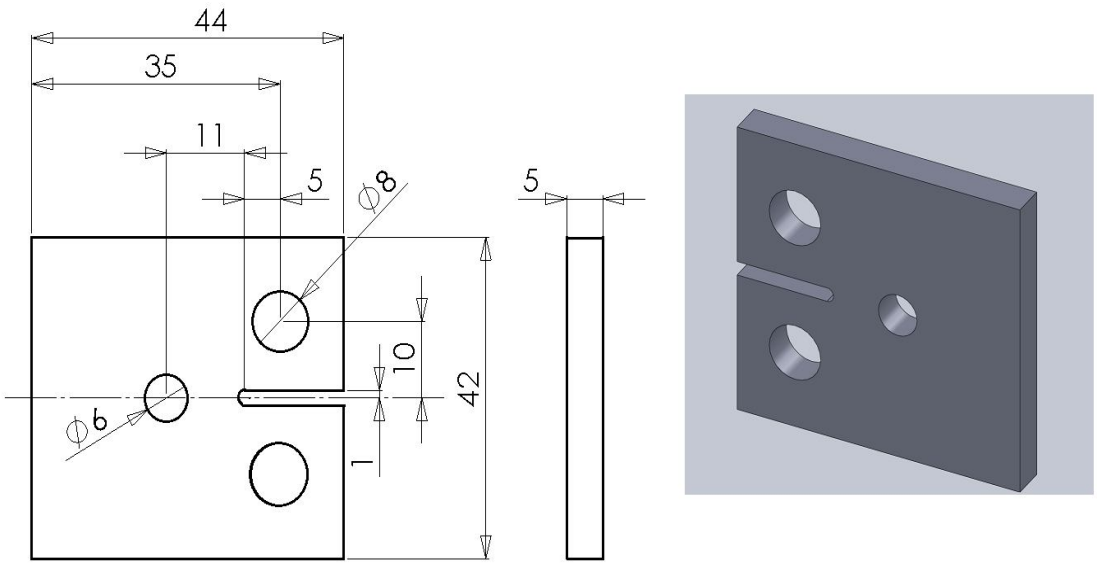

Figure 5.8: Dimensions of the specimens employed for the research and three-dimensional representation obtained with the software SolidWorks.

The starting step of the manufacturing process has been the cutting of the main rectangular bodies of the specimens from the resin plates previously obtained by means of the circular saw of the Institute (Fig.5.9.a). Firstly, the borders of each plate have been removed because of the thickness irregularity due to the adhesion of the molten material to the mould wall. The following cuts have been made having care to not include in the parts any impurity or gas inclusion which could not be removed in subsequent operations and which could hence compromise the utility of the correspondent specimen. The obtained parts have been measured using a digital calliper to detect any inaccuracies of the cuts and sandpaper was used when needed to level the borders.

To create the holes, a vertical drilling machine was used (Fig.5.9.b). Before the placement on the drilling plane, a slight puncture has been performed with a needle in a position corresponding to the centres of the holes, for a more accurate positioning of the drill tips. A proper clamping of the specimens was then essential to avoid vibratory phenomena which would lead to shape irregularities of the holes. In addition, because of the reduced thickness of the element, the drill had to be set to a very high rotational velocity, since a low speed could increase the risk of breakage of the resin part. For creating the small curvature in the internal edge of the notch (see Fig.5.8) a fourth hole has been drilled on the plane of symmetry of the specimen using a 2 mm tip: this device allowed a better precision in the subsequent phase of sawing the notch itself.

Figure 5.9: Machines employed for manufacturing the specimens: a) disc saw; b) vertical drilling machine; c) wet grinder.

A further sawing operation has been thus performed for adding the notches to the specimens. Due to the narrowness of the cut to be done, much attention had to be paid to secure the specimen to the cutting plane and to provide a proper blade thickness of 2 mm. Moreover, since the round shape of the blade could not allow a straight profile of the cut in the length of the thickness, the cutting had to be interrupted before completely reaching the correspondent hole and the operation was then brought on manually using a file.

The subsequent levelling of the thickness to the decided value was performed on the wet grinder of the Institute (Fig. 5.9.c), using two different grades of sandpaper: a coarser one has been employed for reducing the thickness to the final value of 5 mm, while a fine one (grade 1000) has been used to remove scratches and irregularities from the surfaces and the borders. Although the greatest part of the air inclusion has been removed during this operation, and in smaller amount during the previous phases, yet some defects could not be completely eliminated from the specimens bodies. Nevertheless, being their position far from the notched area, they were thought not to compromise the reliability of the upcoming results, since, according to the Linear Elastic Fracture Mechanics (LEFM), the stress distribution during the damaging process is circumscribed to a small area around the crack tip.

Finally, the last step has been the creation of the precrack within the notch of the specimens. To this purpose, a sharp razorblade has been introduced in the notch and slightly hit with a

hammer until its penetration in the material. For a safe handling, the specimens have been firmly clamped with a vice. This method, though not very precise, was successfully brought on until the depth of approximately 2 mm was reached. The completed specimens are shown in Fig. 5.10.

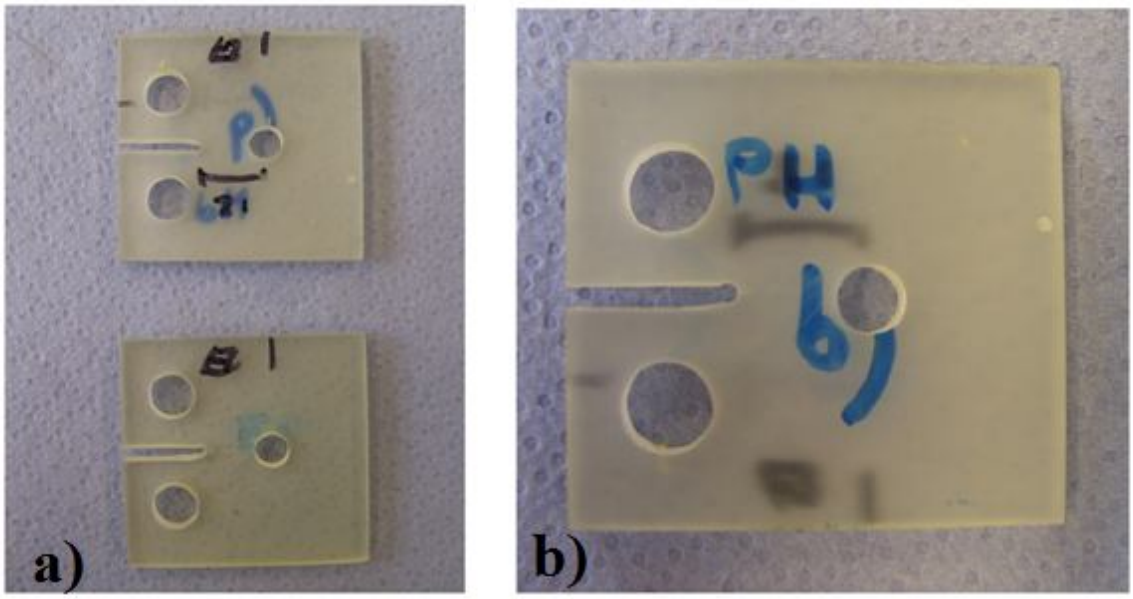

Figure 5.10: Compact Tension specimens at the last stage of the manufacturing process (a). In (b) an air inclusion can be noticed close to the right border, anyway in a position which is not supposed to affect the results of the test.

5.5 Testing of the specimens

After producing a certain number of specimens made of self-healing resin and some others made of unmodified epoxy, prepared for comparison purposes, the experimental phase could be started. As previously explained, the goal has been first to check the effectiveness of the thermoplastic additive, then, in case of positive results, to evaluate the recovery of mechanical strength of the healed material, eventually trying to detect any influence of the number of healing actions and of process parameters such as temperature and duration.

The experimental apparatus consisted in a tensile machine (Zwick/Roell Z 10) operating with position control and in a sensor measuring the displacement between the two halves of the specimen and having the contact points on the edges of the notch (Figg.5.11, 5.12).

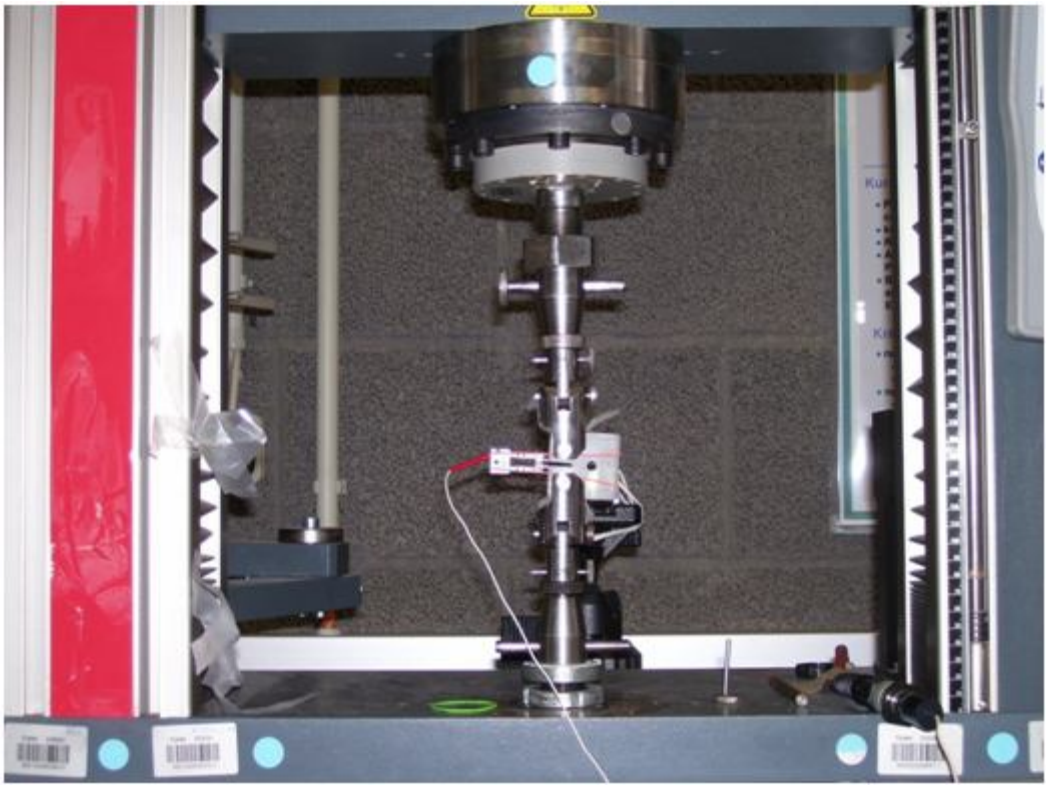

Figure 5.11: Experimental apparatus employed for the performed tests

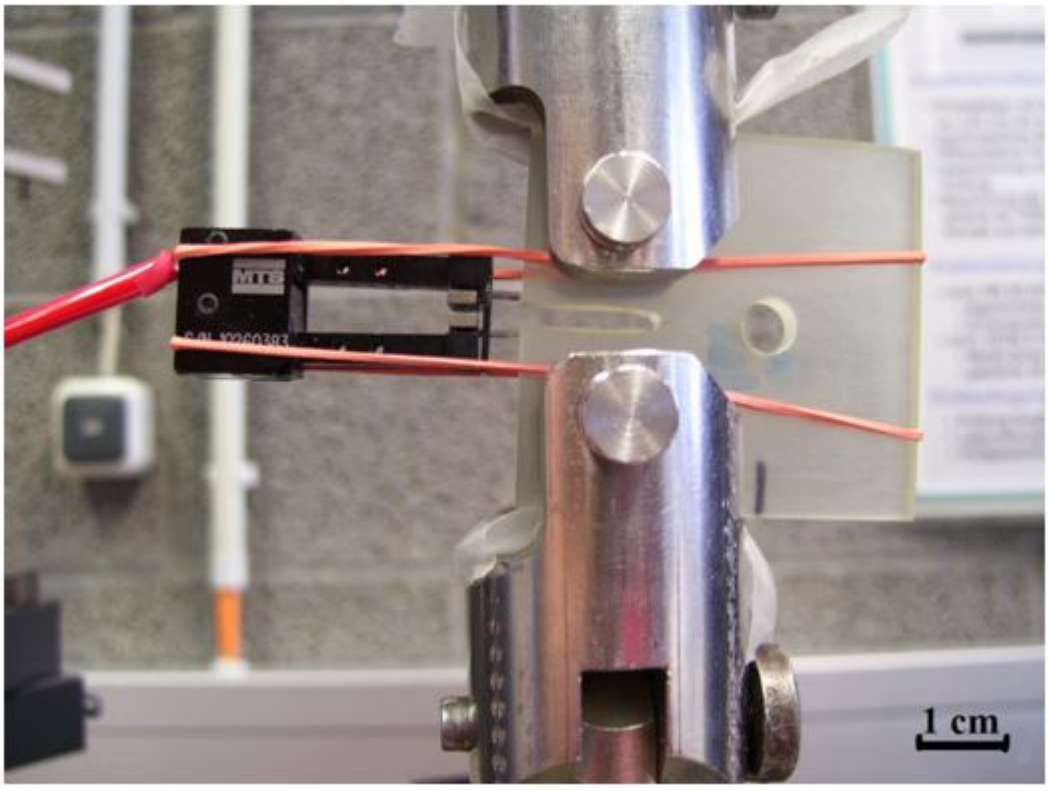

Figure 5.12: : Particular of the sensor and its securing to the specimen.

5.5.1 Calibration of the sensor

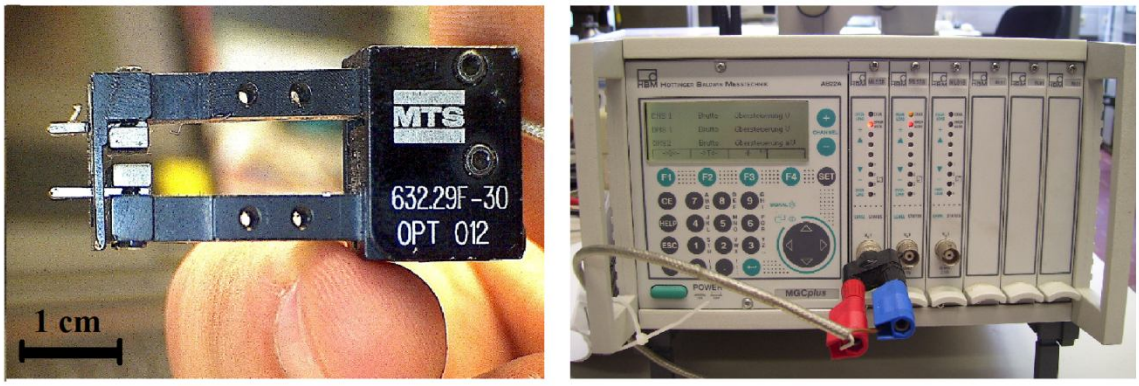

Figure 5.13: a) MTS extensometer used to detect the displacement during the tests; b) control unit used to set the sensor's parameters.

Since the output of the sensor (Fig. 5.13.a) is a variation in voltage, a proper factor had to be obtained for the conversion to a length dimension. To do this, acting on the parameters of the control unit (Fig. 5.13.b), the voltage range was set to a scale from 0 V to 10 V, corresponding respectively to the rest position of the sensor and to its maximum allowed displacement. The values in millimetres were taken by means of a digital calliper. For a better accuracy, being impossible to measure the rest position with a contact instrument without a shifting of the voltage from the null value, a substitutive position, corresponding to the minimum allowed distance between the sensor tips, was considered. Obtaining thus the data reported in Table 5.3, the conversion factor could be easily calculated as the slope m of the resulting graph (Eq.5.1). Moreover, the value at the rest position could be calculated by proportion, thus allowing the calculation of the displacement δ as the product $m \cdot V$.

Table 5.3: Values of voltage and distance between the sensor tips as measured at the limit positions of the moving part.

Position	Measured voltage [V]	Measured distance [mm]
Minimum	- 1.9	3.3
Maximum	10	5.6

$$m = \frac{y_2 - y_1}{x_2 - x_1} = \frac{5.6 - 3.3}{10 + 1.9} = 0.193 \qquad (5.1)$$

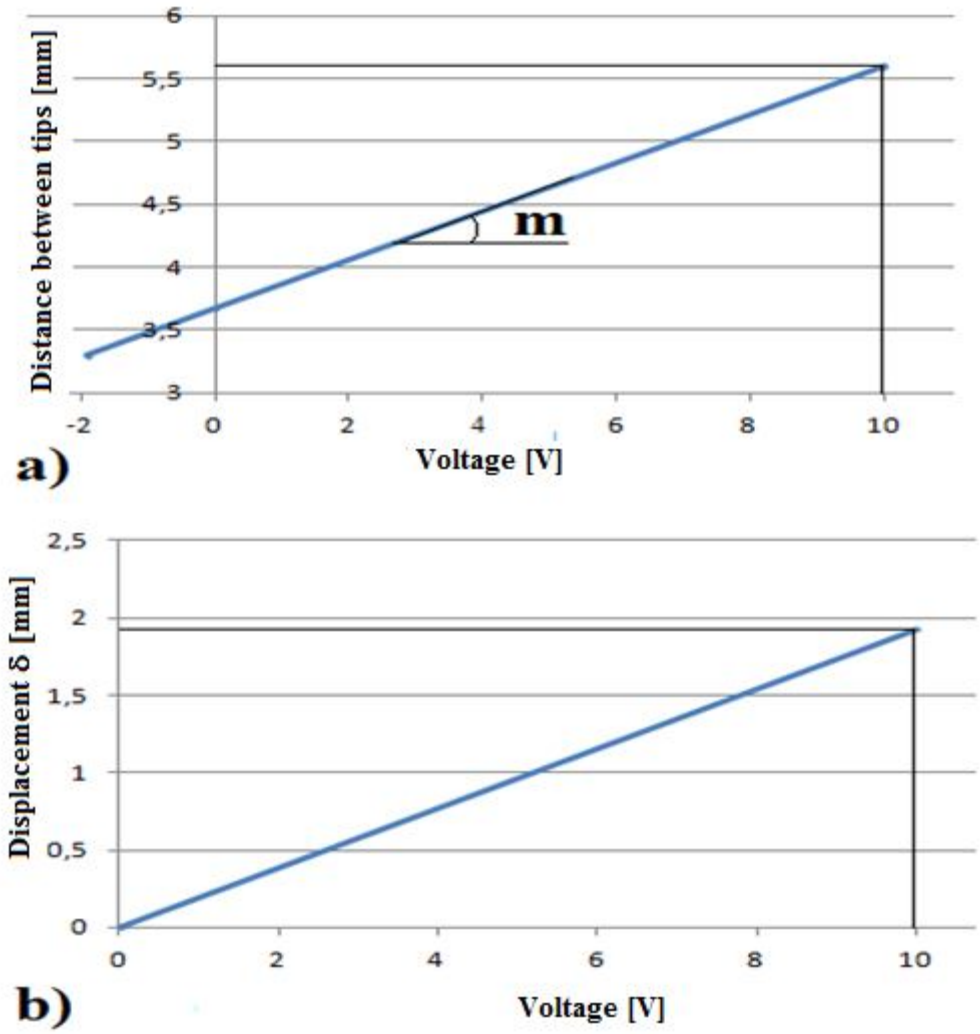

Figure 5.14: a) Relationship between the measured distance of the sensor tips and the correspondent voltage; b) Displacement related to the voltage, the former being obtained setting the origin of the coordinate system to the calculated rest-position value of 3.67 mm.

5.5.2 Performing of the tensile tests

Due to the reduced thickness of the employed specimens, a very careful positioning of the sensor was essential to avoid misplacements during the moving of the machine jaws. The securing has been done by means of a pair of strings, arranged in order to provide a sufficient force on the sensor and prevent it from falling. Moreover, two strips of double-sided adhesive tape was applied on the contact surfaces to avoid the slipping of the sensor tips.

After a proper clamping of the specimen, the tensile tests have been started, having care of setting to zero both the measured force and the voltage before each of them. The machine has been set to a velocity of 1 mm/min for all the tests and the corresponding force was given as output in relationship with the displacement measured by the sensor. It is worth noting that, while in a traditional CT test the failure of the specimen brings a drop to zero of the applied force, a different behaviour was expected when considering a modified specimen with a hole drilled along the path of the propagating crack. In fact, even after the breakage of the portion between the notch and the hole, indicated by a first drop in the force value, yet the null value is not reached, since a residual tensile strength is guaranteed by the remaining unbroken section. For this reason, being the subsequent behaviour not relevant for the actual purposes of the research, each test was interrupted after the occurrence of the first failure, which could be detected visually and by ear.

Once the breakage has occurred and the machine has been blocked, force was newly approached to zero for removing the specimen and starting with the healing process. Immediately after, the specimen has been put into the oven, which had been previously heated up to 100 °C, and left there for a time duration of 1h. To avoid any possible sticking of the material to the base of the oven, a plate covered with a Teflon layer was used as a support. Since theoretically the healing operation could only be successful for a closed crack, that means with the perfect coincidence of the two broken edges, a small vice has been used for applying a compression force on the crack for all the duration of the healing process. Nevertheless, as it resulted from the first test, the heating process proved to somehow influence also the dimension of the clamping holes, since the second clamping of the specimen to the machine pins presented great difficulties and the enlargement of the holes by means of sandpaper was necessary. Thus, to eliminate the problem in the following tests, two M6 bolts (Fig. 5.15) were

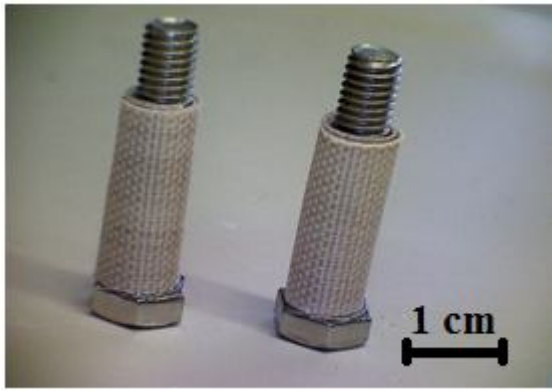

Figure 5.15: Bolts covered with a Teflon layer, employed for preventing the shrinkage of the clamping holes during the heating process.

covered with an adhesive Teflon layer, properly cut to generate a slight interference, and each time inserted in the specimen's holes before the heating phase, to prevent any other shrinkage.

The phases described above have been followed for the greater part of the specimens, performing the heating operation for the time of one hour at 100 °C. In addition to this, since according to previous studies [19] an increase in temperature proved to positively affect the recovery of the material, three of the specimens have been tested supplying heat at the temperature of 130 °C for a time duration of 90 minutes.

5.6 Analysis of results

5.6.1 Influence of the additive

Considering the generally lower mechanical properties of thermoplastic resins when compared to thermosetting ones, the first step of the analysis has been evaluate how the modification of epoxy resin with a phenoxy additive affects the mechanical strength of the resulting matrix system.

To do so, the results coming from the virgin specimens were used to compare the critical load needed to bring to failure the considered specimens. For each set of data, a mean value and a standard deviation were calculated using the following formulas:

Mean value:
$$\bar{x} = \frac{1}{N}\sum_{i=1}^{N} x_i \qquad (5.2)$$

Standard deviation:
$$\sigma_x = \sqrt{\frac{\sum_{i=1}^{N}(x_i - \bar{x})^2}{N}} \qquad (5.3)$$

being *N* the number of the considered elements. The resulting entity of the critical forces and the dispersion of the values are reported in Table 5.4, while a direct comparison is given in Fig. 5.16.

Table 5.4: Critical force and data dispersion for the different sets of specimens.

	Epoxy	Epoxy + PKHB (10 wt%)
Number of specimens	3	7
Mean value for the critical force [N]	221.6	205.8
Standard deviation [N]	21.9	21.6

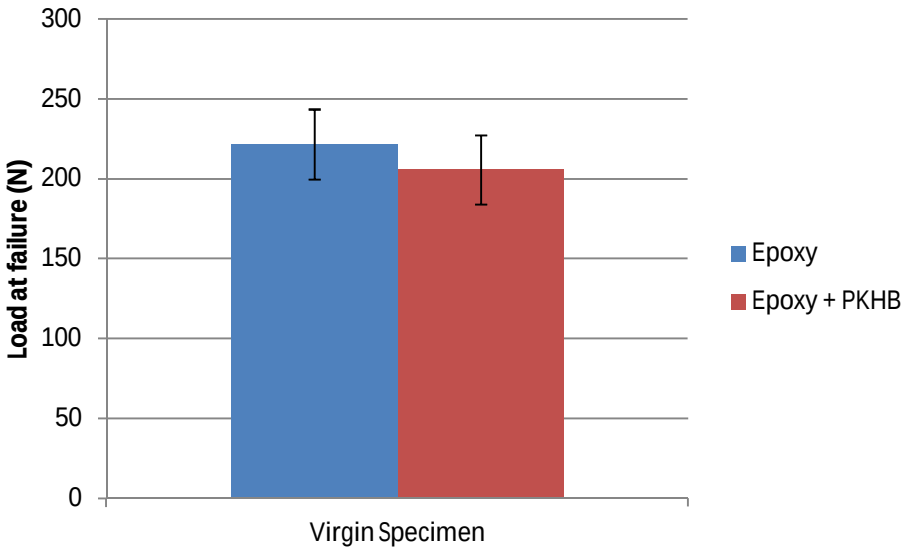

Figure 5.16: Comparison between the critical load of pure epoxy and the same value for the self-healing system.

In addition to this, a comparison between the critical values of the Stress Intensity Factor K_{IC} could be directly obtained from the above reported results. According to the theory, and as reported in the correspondent standards [37], the SIF can be calculated as follows:

$$K_{IC} = f(a/w)\frac{P_C}{h\sqrt{w}} \qquad (5.4)$$

where

P_C is the critical load;

h, w are respectively the thickness and the width of the considered specimen;

$f(a/w)$ is a geometry factor depending from the length of the precrack.

Thus, being the considered specimens characterized by the same geometry and only differing in the employed material, the ratio between the two peak forces can give some information also on how the fracture toughness is affected by the addition of a thermoplastic additive (Eq.5.5).

$$\frac{K_{IC\ (Epoxy+PKHB)}}{K_{IC\ (Epoxy)}} = \frac{P_{C\ (Epoxy*PKHB)}}{P_{C\ (Epoxy)}} = \frac{205.8}{221.6} \approx 0.93 \qquad (5.5)$$

The reported results clearly show how, in spite of a relevant percentage of thermoplastic additive within the matrix system, this seems not to greatly affect the overall strength of the material, which maintains more than the 90 % of its original strength.

5.6.2 Self-healing ability

As previously hinted in Par. 3.3.2, a commonly adopted way to evaluate the self-healing ability of a matrix by means of a CT test is the definition of an efficiency as the ratio between Stress Intensity Factors. Nevertheless, the employment of this method involves the necessity of the difficult calculation of the precrack length on the healed specimen, which is an essential parameter for defining K_{IC}. As seen in Par. 3.3.3, the use of TDCB specimens could solve such problem, since in this case the shape factor *f* of the specimen is no more depending on the crack length, but the more complex geometry would need a too long preparation process. For this reason, new attention was then focused on the possibility of obtaining useful data from simple Compact Tension specimens. The introduction of a new precrack in the healed specimen to recreate the initial conditions of the specimens could not be considered suitable for the purpose: in fact, because of the lower strength detected in the healed area, the hammering of the razor within the notch could not be newly performed without the risk of obtaining a larger extent of the crack. Also, the alternative idea of inserting a Teflon strip to avoid the healing of a two-millimetres-deep section of the crack would necessarily result in an inaccurate coincidence of the edges, compromising the quality of the healing action.

Because of the described difficulties in recreating the initial conditions of the test on the virgin specimens, the former idea of using the peak values of the applied force as a parameter to compare the strengths of the virgin and the healed elements had to be abandoned. Nevertheless, the analysis could be brought on anyway considering the amount of fracture energy *E*

released during the process. This parameter, which is defined as in Eq. 5.6, can be represented as the underlying area of a load-displacement curve (Fig. 5.17):

$$E = \int_0^{x_{lim}} F d\delta \qquad (5.6)$$

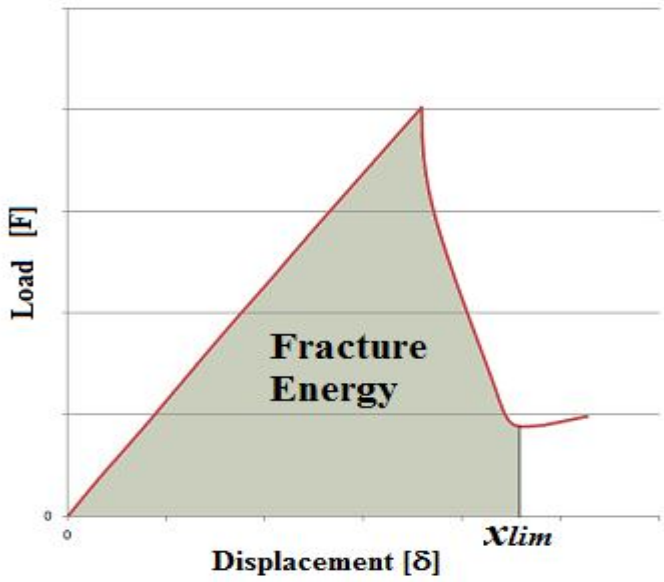

Figure 5.17: Representation of the fracture energy *E* on a load-displacement graph.

According to this, the self-healing ability of the modified resin can be evaluated by a comparison between two areas, obtained from the tests performed respectively on the epoxy and on the epoxy-phenoxy system after the healing action. Since such a comparison does not consider the virgin conditions, in which the notch has been precracked, but only the data coming from two healed specimens, the initial conditions can be assumed as the same and the crack length influences no more the reliability of the results, hence avoiding the difficulties reported above.

The tests performed on unmodified epoxy showed the complete absence of any self-healing phenomena (Fig.5.18): in fact, the data which have been collected during the second test on epoxy specimens, though maintaining a linear trend, show a clearly smaller slope without any sign of discontinuity, highlighting the fact that the cross section of the specimen is markedly reduced already at the very beginning of the tensile action.

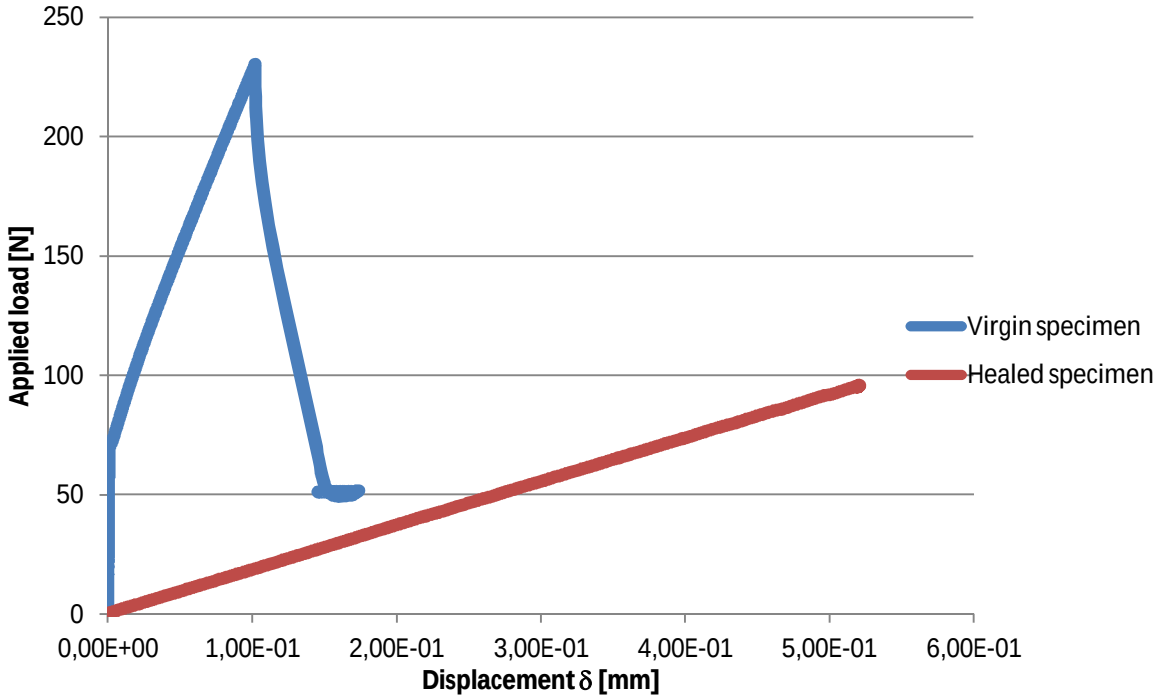

Figure 5.18: First and second tensile tests performed on an epoxy specimen.

Figure 5.19 graphically shows the results coming from tensile tests on modified and unmodified resin after that a first healing process has been performed at the temperature of 100 °C and for a time duration of one hour. In the light of what previously explained, the difference between the areas underlying respectively the green and the red line, considered from the origin to the indicated threshold, represents a gain in the fracture energy needed to bring the healed specimen to failure, thus highlighting a partial recovery of mechanical properties for the modified resin.

Although the closing of the crack could be detected with the naked eye, from a comparison with the values presented in Table 5.4 it becomes clear that the new bonds which create within the crack during the healing action appear to be much weaker than the original ones, with the result of a heavy decrease of the analysed mechanical property. This behaviour could be due to an inadequate pressure on the halves of the crack, since a certain grade of thermal expansion of the metallic vice could not be avoided, or to a sub-optimal choice of parameters for the heating process. Moreover, even the weight ratio of thermoplastic resin added to the blend could be a crucial parameter to achieve a more satisfactory healing.

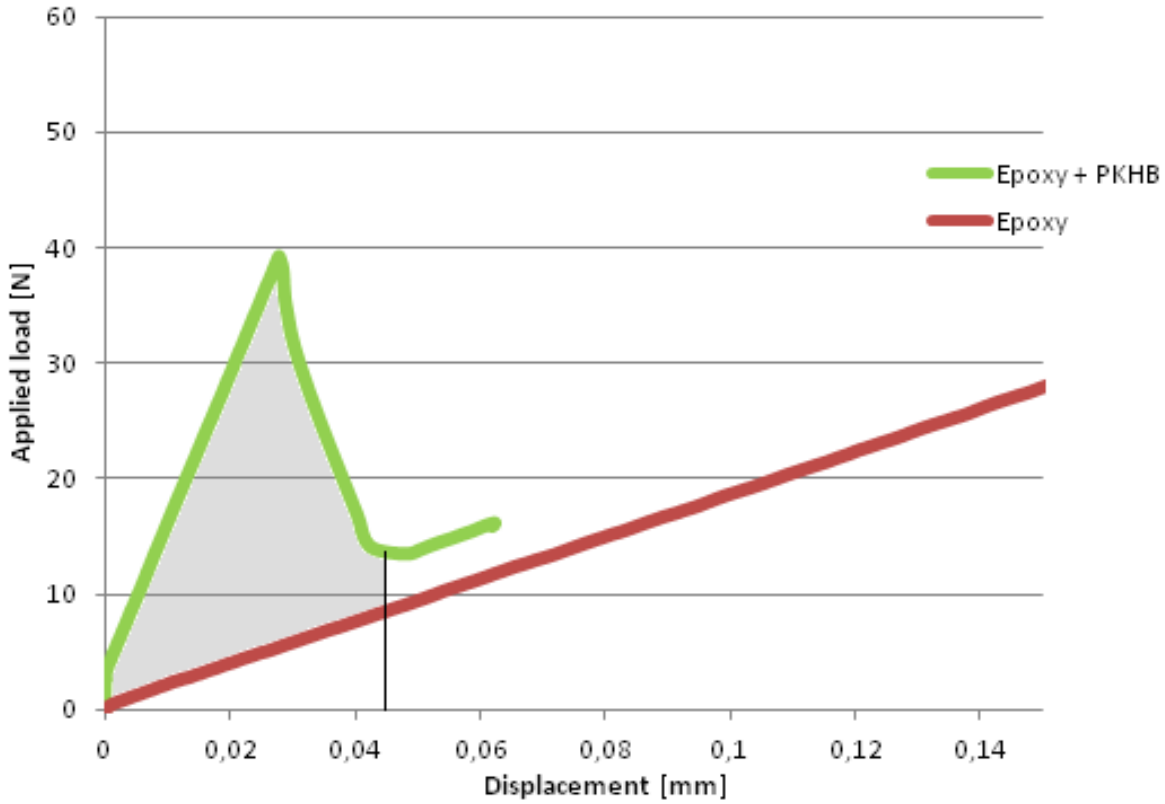

Figure 5.19: Comparison between load-displacement curves for modified and unmodified epoxy after the first healing action (T = 100 °C, t = 60 min.). The grey area represents the gain in fracture energy obtainable with the thermoplastic additive.

5.6.3 Repeatability

One more aspect of the analysis brought on in this work has been to evaluate how the tensile strength could be affected by the number of healing operation performed. In this task, the main difficulty encountered has been the plastic deformation which some of the specimens incurred after multiple healings, making them not suitable for obtaining further reliable results. Nevertheless, three of the specimens could be successfully brought until the fourth tensile test and, although not representing a sufficient number for taking reliable conclusions, the results could be taken as a hint for further experimentation. The load-displacement curves obtained after each healing action on a same specimen are given in Figg. 5.20 and 5.21.

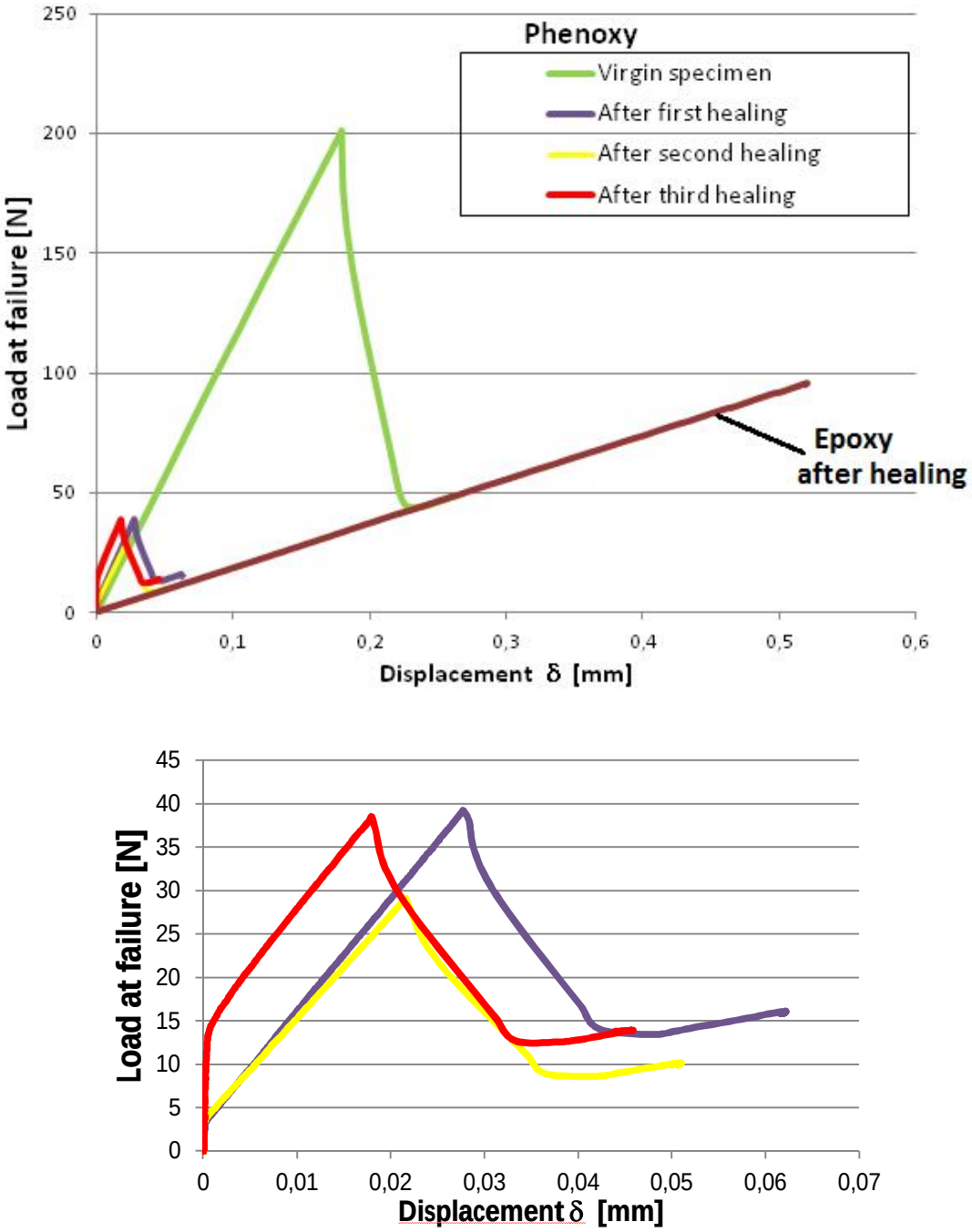

Figure 5.20: Load-displacement curves obtained for subsequent tensile tests on one of the specimens, referred to the curve of the second test on an epoxy specimen.

It can be noticed that, after the first, main drop in strength corresponding to the first healing action, the following data seem to suggest a stabilization of the fracture for the tests performed after the first healing action, with values depending on other parameters than the number of failures. In fact, although the test performed after the second healing is related to a smaller amount of fracture energy (yellow line), the following one shows an evolution which is much more similar to what obtained for the second test (after the first healing action, violet

line). Taking in account that temperature and time duration have been the same for all the healing sessions, these results indicate that the obtainable recovery of the resin system could be depending on the value of the pressure which has been applied to the specimens during the heating operation. Hence, this parameter could be controlled and monitored to get better healing results, though searching for a compromise solution not to provoke permanent distortions on the specimen.

5.6.4 Influence of process parameters

As previously explained, a further set of experiments was brought on in order to verify the better results obtainable with an increase in process parameters as temperature and time duration. The results obtained for two of the specimens after a first healing action performed at 130 °C and for 90 minutes are reported in the following Figure, and compared with their correspondent for a temperature of 100 °C and a time duration of 60 minutes.

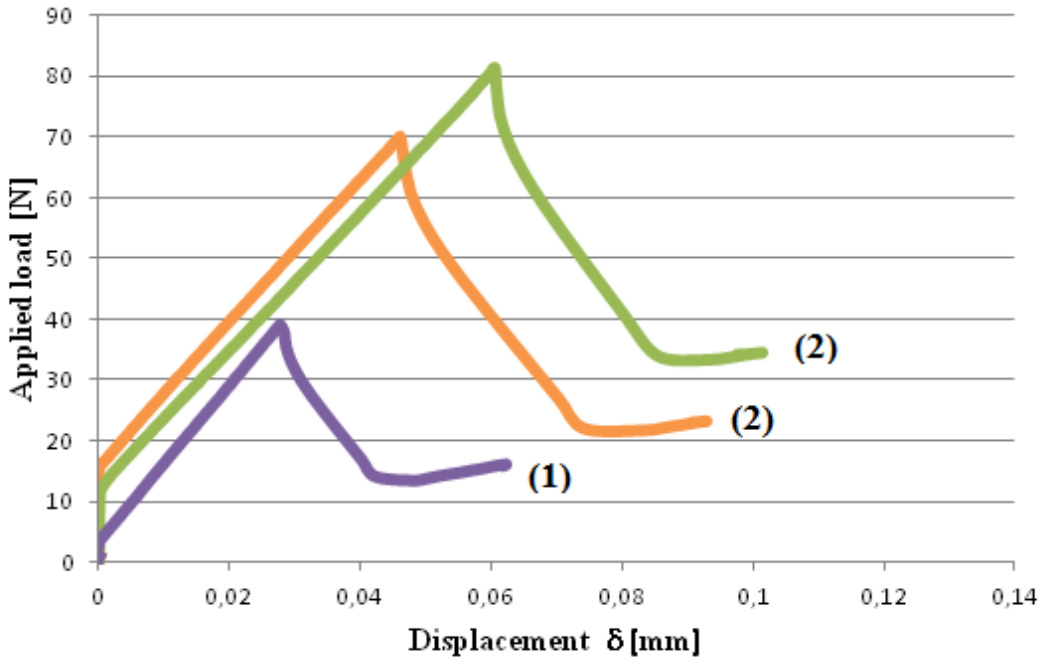

Figure 5.21: Comparison between load-displacement curves obtained after the first healing, performed respectively with T = 100 °C and t = 60 min. (1) and with T = 130 °C and t = 90 min. (2)

As can be detected, the performed tests seem to confirm the expectations, since the area underlying the new graphs is sensibly bigger, thus indicating a gain in fracture energy with higher values of the process parameters. This can be due to a easier diffusion of the thermoplastic additive within the epoxy resin which is obtainable with an increased temperature, while a longer duration of the heat supplying additionally stabilizes the so-created chemical bonds.

5.7 Conclusions and further research

According to the results so far obtained, the system obtained by adding a phenoxy thermoplastic resin to epoxy resin proved to have an actual ability of healing a breakage occurring in the material, provided that the crack edges are in good contact and coincident. In addition to this, the phenomenon of slight shrinkage observed on the clamping holes of the specimens, though not properly investigated, seemed to suggest the possibility of a certain grade of healing also for other kinds of damage which don't allow the complete coincidence of the separate edges.

Nevertheless, in spite of the fact that the occurrence of the closure can be detected to the naked eye, yet the healed part resulted sensibly weaker of the undamaged material, as can be easily noticed comparing the load-displacement curves of a virgin and a healed specimen. Nevertheless, if the damage is repeated, the material seems to preserve its properties of healed resin, at least until the fourth cycle of failure and healing, also with some influence of the applied pressure. In addition to this, the entity of the possible recovery confirmed to be positively influenced by an increase in process parameters such as temperature and time duration. Hence, new studies could be brought on to investigate the eventuality of a limit to this trend other than the degradation temperature of the material and thus outline the optimal features of the healing process.

For what the concentration of healing agent is concerned, the used weight ratio of 10 %, recommended by the producer, seemed not to heavily penalize the strength of the resin system, since the fracture toughness could be preserved at more than 90 % of its former value. Thus, since the main disadvantage of this blend is the low recovery obtained with one healing action, a further research could be focused on testing different mixing ratios to identify the most convenient solution. In addition to this, the manufacturing difficulties encountered in this work, related to the enhanced viscosity of the resin, should be taken in consideration when bringing on the research of the optimal concentration. In particular, the possibility of

using lower additive percentages has to be checked in detail, since a lower viscosity in the resin would make it more suitable for the final goal of producing self-healing composite materials.

Bibliography

[1] http://www.faadooengineers.com/content/297-boeing-787-dreamliner-comes-to-india, accessed on 31.07.12.

[2] Quaresimin, M. : *Introduzione alla progettazione con i materiali compositi*, Padova, 2010.

[3] Montira Sriyai, Master Thesis, Technische Universität Hamburg-Harburg (2008).

[4] Y. C. Yuan, T. Yin, M. Z. Rong, M. Q. Zhang: *Self healing in polymer and polymer composites. Concept, realization and outlook, a review*, eXPRESS Polymer Letters Vol.2, No.4 (2008) 238–250.

[5] S. R. White, N. R. Sottos, P. H. Geubelle, J. S. Moore, M. R. Kessler, S. R. Sriram, E. N. Brown, S. Viswanathan: *Autonomic healing of polymer composites*, Nature vol.409 (2001), 794-797.

[6] H.M. Andersson, MW Keller, JS Moore, NR Sottos, SR White: *Self Healing Polymers and Composites*, from "Self Healing Materials. An Alternative Approach to 20 Centuries of Materials Science", Springer (2007) 19–44.

[7] M.W. Keller, N.R. Sottos: *Effect of microcapsule properties on self-healing composite performance.*

[8] S. M. Bleay, C. B. Loader, V. J. Hawyes, L. Humberstone, P.T.Curtis: *A smart repair system for polymer matrix composites*, Composites: Part A 32(2001) 1767-1776.

[9] Dry C, McMillan W.: *Three-part methylmethacrylate adhesive system as an internal delivery system for smart responsive concrete*, Smart Mater Struct 1995;5(3):297-300.

[10] Jody W.C. Pang, Ian P. Bond: *A hollow fibre reinforced polymer composite encompassing self-healing and enhanced damage visibility*, Composites Science and Technology 65 (2005) 1791–1799.

[11] M. Motuku, U. K. Vaidya, G. M. Janowski: *Parametric studies on self-repairing approaches for resin infused composites subjected to low velocity impact*, Smart Mater. Struct. 8 (1999) 623–638.

[12] M. Castellucci: *Resistive Heating for Self-healing Materials Based on Ionomeric Polymers* (2009).

[13] Ian P. Bond, Richard S. Trask, Hugo R. Williams, Gareth J. Williams: *Self Healing Fibre-reinforced Polymer Composites: an Overview*, from "Self Healing Materials. An Alternative Approach to 20 Centuries of Materials Science", Springer (2007) 115-138.

[14] Toohey K. S., Sottos N. R., Lewis J. A., Moore J. S.,White S. R.: *Self-healing materials with microvascular networks,* Nature Materials, 6, 581–585 (2007).

[15] B.J. Blaiszik, S.L.B. Kramer, S.C. Olugebefola, J.S. Moore, N.R. Sottos, S.R. White: *Self-Healing Polymers and Composites*, Annu. Rev. Mater. Res. 2010.40:179-211.

[16] Peterson AM, Jensen RE, Palmese GR.: *Reversibly cross-linked polymer gels as healing agents for epoxy-amine thermosets*, (2009) Appl. Mater. Interfaces 1(5):992–95.

[17] A. Peterson: *Development of Remendable Materials Using Reversible Bonds*, http://www.chemeng.drexel.edu/palmesegroup/research/peterson/default.aspx , accessed on 05.04.2012.

[18] Chen X., Dam M. A., Ono K., Mal A., Shen H., Nutt S. R., Sheran K., Wudl F.: *A thermally re-mendable cross-linked polymeric material*, Science, 295, 1698–1702 (2002).

[19] S.A. Hayes, F.R. Jones, K. Marshiya, W. Zhang: *A self-healing thermosetting composite material*, Composites: Part A 38 (2007) 1116–1120.

[20] S.A Hayes, W Zhang, M Branthwaite, and F.R Jones: *Self-healing of damage in fibre-reinforced polymer-matrix composites*, J R Soc Interface. 2007 April 22; 4(13): 381–387.

[21] F.R. Jones, W. Zhang, S.A. Hayes: *Thermally Induced Self Healing of Thermosetting Resins and Matrices in Smart Composites*, , from "Self Healing Materials. An Alternative Approach to 20 Centuries of Materials Science", Springer (2007), 69-93.

[22] Xiaofan Luo, Runqing Ou, Daniel E. Eberly, Amit Singhal, Wantinee Viratyaporn, Patrick T. Mather: *A Thermoplastic/Thermoset Blend Exhibiting Thermal Mending and Reversible Adhesion,* Applied Materials and Interfaces, vol. I n.3 (2009) 612-620.

[23] Martin R. Tant, Garth L. Wilkes (1988): *An Overview of the Viscous and Viscoelastic Behavior of Ionomers in Bulk and Solution*, Journal of Macromolecular Science, Part C: Polymer Reviews, 28:1, 1-63.

[24] A, Eisenberg, M. Rinaudo: *Polyelectrolytes and ionomers***,** Polymer Bulletin 24, 671 (1990).

[25] A. Eisenberg, B. Hird, R. B. Moore: *A New Multiplet-Cluster Model for the Morphology of Random Ionomers*, Macromolecules 1990, 23, 4098-4107.

[26] Kenji Tadano, Eisaku Hirasawa, Hitoshi Yamamoto, Shinichi Yano: *Order-Disorder Transition of Ionic Clusters in Ionomers*, Macromolecules 1989, 22, 226-233.

[27] R. Fall: *Puncture Reversal of Ethylene Ionomers – Mechanistic Studies*, Master Thesis, Virginia Polytechnic Institute and State University (2001).

[28] S.J. Kalista Jr. : *Self-Healing of Thermoplastic Poly(Ethylene-co-Methacrylic Acid) Copolymers Following Projectile Puncture*, Master Thesis, Virginia Polytechnic Institute and State University (2003).

[29] R. Varley: *Ionomers as Self Healing Polymers*, from "Self Healing Materials. An Alternative Approach to 20 Centuries of Materials Science", Springer (2007), 95–114.

[30] R.l J. Varley, S. van der Zwaag: *Towards an understanding of thermally activated self-healing of an ionomer system during ballistic penetration*, Acta Materialia 56 (2008) 5737–5750.

[31] British Standards (BS), Standard BS ISO 15850:2002, *Plastics - determination of tension-tension fatigue crack propagation – Linear Elastic Fracture Mechanics (LEFM) approach* (2012).

[32] E. N. Brown: *Use of the tapered double cantilever beam geometry for fracture toughness measurements and its application to the quantification of self-healing*, The Journal of Strain Analysis for Engineering Design 2011 46: 167.

[33] Data Sheet for Surlyn® 8940, DuPont Packaging & Industrial Polymers, http://www2.dupont.com/Surlyn/en_US/assets/downloads/surlyn_8940.pdf (09.08.12).

[34] *Material Safety Data Sheet for Araldite LY 1556*, Huntsman AM, http://www.nfgsales.com/files/active/0/Araldite%20LY%201556%2005_19_10.pdf (09.08.12).

[35] Data Sheet of matrix systems for industrial composites, *Araldite® LY 1556 / Aradur® 1571 / Accelerator 1573 / Hardener XB 3403,* https://www.huntsmanservice.com/WebFolder/ui/browse.do?pFileName=/opt/TDS/Huntsman%20Advanced%20Materials/English/Long/Araldite%20LY%201556_Aradur%201571_Accelerator%201573_Hardener%20XB%203403_eur_e.pdf (09.08.12).

[36] Typical properties for PKHB phenoxy, InChem website http://phenoxy.com/ products/pkhb_.html (09.08.12) .

[37] British Standards (BS), Standard BS ISO 13586:2000, *Plastics – Determination of fracture toughness (G_{IC} and K_{IC}) – Linear Elastic Fracture Mechanics (LEFM) approach (2012).*